

Discovery of AMG 925, a FLT3 and CDK4 Dual Kinase Inhibitor with Preferential Affinity for the Activated State of FLT3

Zhihong Li,^{*,†} Xianghong Wang,[†] John Eksterowicz,[†] Michael W. Gribble, Jr.,[†] Grace Q. Alba,[§] Merrill Ayres,[†] Timothy J. Carlson,^{||} Ada Chen,[†] Xiaoqi Chen,[†] Robert Cho,^{||} Richard V. Connors,[†] Michael DeGraffenreid,[†] Jeffrey T. Deignan,[†] Jason Duquette,[†] Pingchen Fan,[†] Benjamin Fisher,[†] Jiasheng Fu,[†] Justin N. Huard,[⊥] Jacob Kaizerman,[†] Kathleen S. Keegan,[⊥] Cong Li,[‡] Kexue Li,[†] Yunxiao Li,[†] Lingming Liang,[‡] Wen Liu,[†] Sarah E. Lively,[†] Mei-Chu Lo,[†] Ji Ma,^{||} Dustin L. McMinn,[†] Jeffrey T. Mihalic,[†] Kriti Modi,[†] Rachel Ngo,[†] Kanaka Pattabiraman,[†] Derek E. Piper,[†] Christophe Queva,[⊥] Mark L. Ragains,[§] Julia Suchomel,[†] Steve Thibault,[†] Nigel Walker,[†] Xiaodong Wang,[†] Zhulun Wang,[†] Malgorzata Wanska,[†] Paul M. Wehn,[†] Margaret F. Weidner,[⊥] Alex J. Zhang,[†] Xiaoning Zhao,[†] Alexander Kamb,[#] Dineli Wickramasinghe,[‡] Kang Dai,[‡] Lawrence R. McGee,[†] and Julio C. Medina[†]

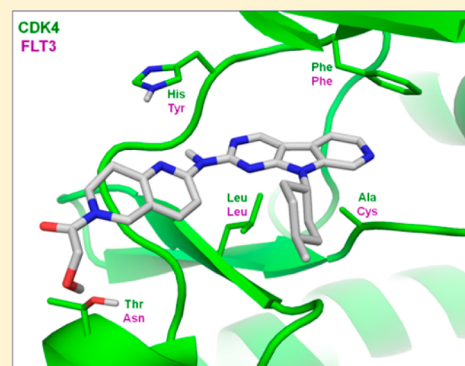
Departments of [†]Therapeutic Discovery, [‡]Oncology Research, [§]Pharmaceutics, and ^{||}Pharmacokinetics and Drug Metabolism, Amgen Inc., 1120 Veterans Boulevard, South San Francisco, California 94080, United States

[⊥]Therapeutic Innovation Unit, Amgen Inc., 1201 Amgen Court West, Seattle, Washington 98119, United States

[#]Discovery Research, Amgen Inc., One Amgen Center Drive, Thousand Oaks, California 91320, United States

Supporting Information

ABSTRACT: We describe the structural optimization of a lead compound **1** that exhibits dual inhibitory activities against FLT3 and CDK4. A series of pyrido[4',3':4,5]pyrrolo[2,3-d]pyrimidine derivatives was synthesized, and SAR analysis, using cell-based assays, led to the discovery of **28** (AMG 925), a potent and orally bioavailable dual inhibitor of CDK4 and FLT3, including many FLT3 mutants reported to date. Compound **28** inhibits the proliferation of a panel of human tumor cell lines including Colo205 (Rb⁺) and U937 (FLT3^{WT}) and induced cell death in MOLM13 (FLT3^{ITD}) and even in MOLM13 (FLT3^{ITD, D835Y}), which exhibits resistance to a number of FLT3 inhibitors currently under clinical development. At well-tolerated doses, compound **28** leads to significant growth inhibition of MOLM13 xenografts in nude mice, and the activity correlates with inhibition of STAT5 and Rb phosphorylation.



INTRODUCTION

Acute myeloid leukemia (AML) is a grievous disease for which there is significant unmet medical need. There are 14600 cases diagnosed each year, with an estimated 10400 deaths in the U.S. alone.¹ The standard of care for AML is poorly tolerated among elderly patients. Durable responses are also lacking, and rapid relapse is common. FMS-like tyrosine kinase 3 (FLT3) belongs to the receptor tyrosine kinase class III family and is expressed at high levels in most clinical samples from AML and B-precursor acute lymphoblastic leukemia (ALL) patients.^{2–4} Activating mutations in FLT3, mostly internal tandem duplication (ITD), are detected in approximately 30% of AML patients and are associated with poor prognosis.⁵ The important role that FLT3 plays in the survival and proliferation of AML blast through the STAT5, RAS-ERK, and phosphatidylinositol 3 kinase (PI3K) signaling pathways, as well as its mutation and overexpression in large numbers of AML patients, make FLT3 a particularly attractive target for AML therapy.⁶

Despite extensive efforts toward developing targeted agents for treatment of AML,⁷ a critical unmet need remains. FLT3 tyrosine kinase inhibitors used as monotherapies for AML have effected reductions in peripheral blood and bone marrow blasts in only a minority of AML patients, and these effects have usually been transient. This may be due to selection of drug-resistant mutants which are the primary resistance mechanism observed in the clinic,⁸ increases in FLT3 expression during treatment, or activation of other signaling pathways.⁹

Cyclin-dependent kinase 4 (CDK4), which is downstream of FLT3¹⁰ and other growth signaling pathways, is also up-regulated in AML by overexpression of cyclin D through activation of tyrosine kinase growth signaling pathways and loss of p15 inhibitory function.¹¹ Misregulated CDKs cause uncontrolled proliferation as well as genomic and chromosomal

Received: January 22, 2014

Published: March 18, 2014

instability.¹² In addition, synergistic activity has been observed in preclinical studies when FLT3 and CDK4 were inhibited in AML cell lines.¹⁰

These findings together suggest the potential for a FLT3/CDK4 dual inhibitor to provide significant benefit in the treatment of AML, including improving durability of clinical response by simultaneously modulating two synergistic and commonly dysregulated targets.

RESULTS AND DISCUSSION

Previously, we reported the discovery of substituted pyrido[4',3':4,5]pyrrolo[2,3-*d*]pyrimidine **1** (Figure 1) as a novel

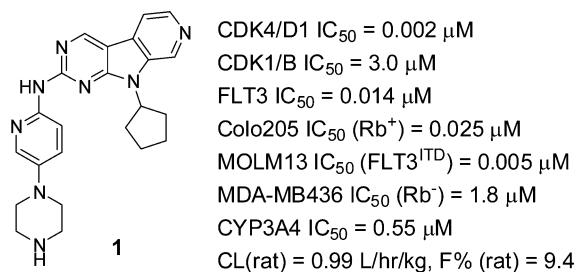


Figure 1. Lead compound **1**.

CDK4/6 inhibitor.¹³ During kinase profiling it was found that compound **1** also inhibits FLT3, yet possesses promising selectivity against other kinases. This finding can be rationalized on the basis of the high degree of similarity between the binding domains of CDK4/6 (co-crystal structure of CDK6 with **1** in Figure 2a) and APO FLT3 (modeled with **1** in Figure

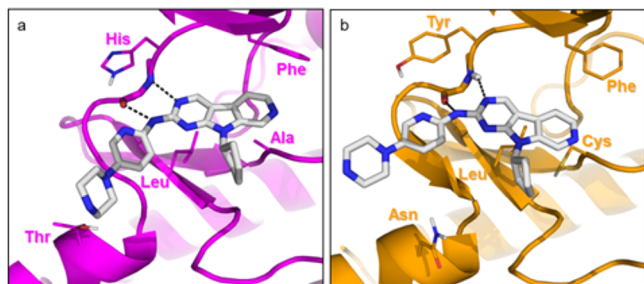


Figure 2. Binding of compound **1** in CDK6 and FLT3. (a) Co-crystal structure of compound **1** in CDK6 at 2.9 Å resolution (PDB code 4P41). (b) Compound **1** with homology model of FLT3.¹⁴ The key active site residues are highlighted in stick representation.

2b). The active sites of the two enzymes differ by only a few residues, and the binding mode of **1** obtained by modeling with FLT3 very closely resembles that observed in the co-crystal structure with CDK6.

In both structures, the fused pyridine moiety of the inhibitor engages the phenylalanine gatekeeper residue in an edge-to-face interaction, while the aminopyrimidine ring system participates in two hydrogen bonding interactions with residues in the hinge loop. In both structures, the cyclopentyl group sits in a small hydrophobic cleft between a leucine floor residue and small side chain alanine (CDK4) or cysteine (FLT3). Taking advantage of these shared structural features and binding interactions, we sought to develop dual kinase inhibitors of FLT3/CDK4 for the treatment of AML.

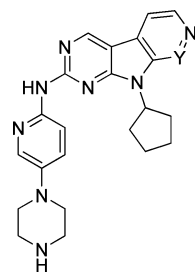
Lead optimization was conducted to address three main issues associated with **1**: CYP3A4 inhibition, suboptimal

selectivity, and poor oral bioavailability. For structure–activity relationship (SAR) analysis, FLT3 and CDK family kinases assays were used as a primary screen to monitor on/off target activities, with the hope that the selectivity within the CDK family may be reflective of broader kinase selectivity. The selectivity over CDK1 is necessary for reducing toxicity and confounding in vivo analysis.^{11,15} Using biochemical assays to optimize against 500 kinases was deemed impractical, therefore cell-based FLT3 and CDK4 specific assays were used for screening inhibitors. Three tumor cell lines, Colo205, MOLM13, and MDA-MB436, were chosen. Colo205 is a human colorectal cancer cell line whose viability depends on the activation of the cyclin D-CDK4-Rb pathway. MOLM13 is a human AML cell line whose viability depends on a constitutively activated FLT3 kinase. MDA-MB436 is a human breast cancer cell line whose viability is independent of FLT3 and CDK4 and was thus included to monitor for off-target effects. Compounds were anticipated to be selective if they had high potency against MOLM13 and Colo205 cells but low activity against MDA-MB436 cell line.

While the CYP3A4 inhibitory activity of the lead **1** stems from the fused pyridine ring of the tricyclic core, our earlier SAR studies¹³ had established that this feature was critical for maintaining good cellular potency. Our strategy for attenuating the CYP3A4 inhibition, therefore sought not to eliminate this feature but rather to modulate its ability to coordinate heme iron through introduction of either sterically demanding or electron-withdrawing substituents *ortho* to the pyridine nitrogen (Table 1). The applicability of this strategy quickly proved limited, however, as only small substituents, such as chloro or methyl, were tolerated by the kinases. While these changes effectively eliminated the CYP3A4 inhibition, they diminished either cellular or enzymatic potency and in some cases incurred potential cardiovascular liabilities by markedly increasing affinity for the hERG ion channel.

Thus, substitution with fluoro or chloro maintained enzymatic potency and selectivity but resulted in reduced cellular potencies and unacceptably high affinities for hERG (**2** and **3**, hERG IC₅₀ = 0.72, 2.0 μM, respectively). Additionally, these halopyridine analogues suffered from increased clearances in rat (from 0.98 L/h/kg for **1** to 2.1 L/h/kg for **2** and 1.7 L/h/kg for **3**). Substitution with methyl and hydroxyl groups (**4** and **5**) maintained cellular potency against MOLM13 but significantly decreased the CDK4-related activity against Colo205 cells. Substitution with a cyano group (**6**) resulted in decreased potency for both CDK4 and FLT3. Replacement of the pyridine ring with a fused pyridazine (**7**) likewise eliminated CYP3A4 inhibition at the expense of potency and pharmacokinetic properties (rat CL = 5.6 L/h/kg). The pyridine-modification strategy for attenuating CYP3A4 inhibition was deemed at this point to be very challenging. One after another, new analogues reinforced the view of the unsubstituted pyridine of **1** as critical for potency and physicochemical and pharmacokinetic properties.

As we explored additional SAR of the cycloalkane moiety, we noticed an opportunity for attenuating CYP3A4 inhibition through remote influences on the heme iron coordination sphere. The cyclopentane ring of **1** occupies a region of the kinases known as the sugar pocket, where the ribose moiety of ATP normally binds. The sugar pockets of CDK4 and FLT3 are formed by both polar and nonpolar residues, with the more deeply buried region of the pocket being hydrophobic in character and surrounded by a solvent exposed, polar rim

Table 1. Modification of the Fused Pyridine Ring^a

Y	1 CH	2 CF	3 CCl	4 CCH ₃	5 COH	6 CCN	7 N
CDK4/D1 IC ₅₀ (μM)	0.003	0.003	0.004	0.020	0.005	0.027	0.051
FLT3 IC ₅₀ (μM)	0.014	0.011	0.005	0.022	0.017	0.046	0.095
CDK1/B IC ₅₀ (μM)	3.00	7.56	3.30	2.26	10.0	30.0	4.78
Colo205 IC ₅₀ (μM)	0.025	0.052	0.063	0.28	0.12	0.35	0.051
MOLM13 IC ₅₀ (μM)	0.005	0.021	0.009	0.005	0.005	0.062	ND
MDA-MB436 IC ₅₀ (μM)	1.76	2.61	2.10	3.42	2.10	1.38	7.05
CYP3A4 INH% _{@3} μM	90	<10	<10	<10	18	ND	<10
CYP3A4 IC ₅₀ (μM)	0.55	>10	>10	>10			>10
Rat CL (L/h/kg)	0.99	2.1	1.7	ND	ND	ND	5.6

^aValues were the means of at least three determinations; standard deviation was ±30%. ND: not determined.

(Figure 3). These amphipathic pockets can accommodate a variety of cyclic moieties, including rings substituted with either

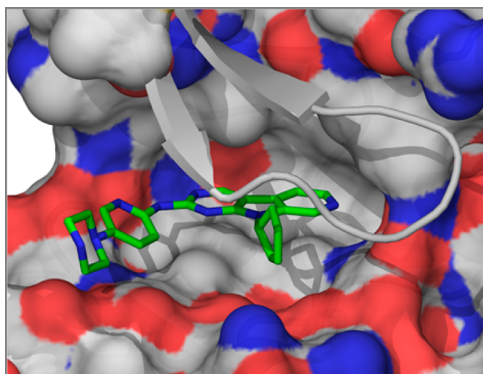


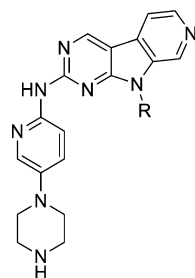
Figure 3. CDK6/compound 1 co-crystal structure highlighting ATP binding site with P-loop surface removed for clarity (PDB code 4P41).

polar or nonpolar groups. We also considered the complementary possibility that replacing the cyclopentyl ring with a polar surrogate could impact CYP3A4 inhibition by changing the physicochemical properties of the molecule. Extensive exploration of this region was performed, and only selected examples are discussed here (Table 2).

As evidenced by compound **8**, an acyclic moiety containing a polar group can significantly reduce CYP3A4 inhibition; however, in most cases this modification resulted in a more than 10-fold loss of the binding affinity to the kinase target. However, the hydroxyl substituted cyclohexane (**9**) did not significantly reduce CYP3A4 inhibition and additionally suffered losses of cellular potency and selectivity relative to **1**. Likewise, bulkier aliphatic rings, like cyclohexyl (**10**) and cycloheptyl (data not shown), did not modulate CYP3A4 inhibitory activity either. However, addition of a methyl group at the 4-position of the cyclohexyl moiety led to a significant reduction in CYP3A4 inhibition (**11**). Entry **11** corresponds to a mixture of *cis* and *trans* diastereomers (1/1 ratio), and based on data collected from previous analogues, we predicted that

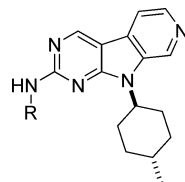
the *trans*-isomer was responsible for the decreased affinity for CYP3A4. Subsequently, the *trans*-isomer (**12**) was prepared in stereochemically pure form and found to be free of this liability (CYP3A4 IC₅₀ >10 μM). Docking studies¹⁶ of a series of inhibitors in the active site of CYP3A4 supported the hypothesis that ligation of the heme iron could be disfavored by a remote steric interaction with a sterically bulky cycloalkane. While the studies revealed favorable binding modes associated with coordination of the heme iron by the pyridine moiety of **1**, steric interactions developed between the cycloalkane and key residues of the CYP active site when the cycloalkane was appropriately substituted, and these destabilizing interactions grew more pronounced as the substituent was made longer and bulkier. Compound **14** illustrates that this effect does not derive from nonspecific lipophilicity but requires the specific steric demand available in compounds **12** and **13**. As the *trans*-4-methylcyclohexyl group abolished CYP3A4 inhibition without diminishing FLT3 or CDK4 potency or inducing any other known liabilities, this group was chosen for further analogues.

Having overcome one of the three major challenges associated with this series by optimizing the tricyclic core and its cycloalkyl substituent, we next sought to improve bioavailability and FLT3 potency through appropriate modifications of the distal amine function (i.e., the piperazine ring of **1**) and the heteroarene ring linking it to the tricyclic core. In the co-crystal structure, the piperazine ring sits in a channel of the kinase that opens toward solvent and can accommodate a wide array of polar groups. We therefore anticipated that optimization of the physicochemical properties of the dual inhibitors by variation of the pyridinylpiperazine could be especially fruitful. Our initial work focused on developing a series that retained a basic amine because this feature was known to contribute favorably to selectivity within the CDK family and to solubility. The piperazine basic nitrogen of **1**, which is protonated under physiological conditions, rests above a threonine residue in the X-ray co-crystal structure with CDK6 (Thr-102 in CDK4) and engages this residue in a hydrogen-bond interaction (Figure 2), whereas the corresponding lysine-

Table 2. Optimization of the Sugar Pocket Binding Moiety^a

	8	9	10	11	12	13	14
R							
CDK4/D1 IC ₅₀ (μM)	0.040	0.003	0.005	0.001	0.007	0.001	0.003
FLT3 IC ₅₀ (μM)	0.043	0.005	0.002	0.002	0.002	0.017	0.003
CDK1/B IC ₅₀ (μM)	12.8	3.41	6.53	5.20	2.66	2.91	2.96
Colo205 IC ₅₀ (μM)	1.24	0.066	0.032	0.055	0.020	0.028	0.033
MOLM13 IC ₅₀ (μM)	ND	0.025	ND	ND	0.013	0.035	0.010
MDA-MB436 IC ₅₀ (μM)	30.0	2.61	0.54	1.02	1.21	2.01	1.62
CYP3A4 INH% _{@3μM}	17	70	82	46	20	51	90
CYP3A4 IC ₅₀ (μM)	> 10				>10	9.5	

^aValues were the means of at least three determinations; standard deviation was ±30%. ND: not determined.

Table 3. Optimization of the Heteroaryl Linker^a

	15	16	17	18	19	20	21
R							
CDK4/D1 IC ₅₀ (μM)	0.003	0.002	0.002	0.002	0.002	0.001	0.003
FLT3 IC ₅₀ (μM)	0.0003	0.006	0.001	0.002	0.004	0.0006	0.0002
CDK1/B IC ₅₀ (μM)	0.024	1.53	0.41	3.29	2.20	2.68	0.79
Colo205 IC ₅₀ (μM)	0.007	0.022	0.005	0.010	0.011	0.016	0.054
MOLM13 IC ₅₀ (μM)	0.005	0.013	0.008	0.010	0.009	0.013	0.002
MDA-MB436 IC ₅₀ (μM)	0.038	1.01	1.20	1.25	2.15	1.47	1.12
Rat CL (L/h/kg)	ND	0.35	ND	2.1	0.61	1.2	0.55
F (% _{rat}) ^b	ND	11	ND	44	28	88	62

^aValues were the means of at least three determinations; standard deviation was ±30%. ^bFormulation: 1.5% sodium acetate/pH4. ND: not determined.

89 of CDK1 should interact unfavorably with the basic amine function.

Extending the basic nitrogen farther into the solvent channel by making it exocyclic (**17**) (Table 3) substantially increased cellular and FLT3 potency but diminished selectivity for CDK4 over CDK1 compared to **12**. Selectivity for CDK4 was restored when the primary amine of **17** was bis-methylated (**18**) while maintaining similar potency across the biochemical and cellular assays.

In parallel with these studies, we also explored the effects of atom substitution within the heteroarene linker (**15**, **16**, **19**, **22–25**) (Tables 3 and 4) as well as installation of an additional substituent *ortho* to the pyridine nitrogen (**20**, **21**, **27**, **28**). Transposing the pyridine nitrogen markedly improved potency against FLT3 but severely eroded selectivity within the CDK family (**12** versus **15**). Replacing the pyridine with a more polar pyridazine (**16**, **19**, **22–25**) did not affect potency or selectivity but did favorably impact a number of important pharmacokinetic parameters such as solubility and bioavailability. Unexpectedly, heteroatom substitution *ortho* to the pyridine nitrogen gave remarkable increases in FLT3 potencies (picomolar IC_{50} s for **20**, **21**) and dramatic improvements in oral bioavailability while maintaining acceptable selectivity among the CDKs. Unfortunately, these compounds were not tolerated in mice at doses that led to 100% tumor growth inhibition (TGI) in xenograft studies.

Convergence of the heteroarene and distal amine-modification strategies resulted in compound **19** (CDK4 IC_{50} = 2 nM; FLT3 IC_{50} = 4 nM; MOLM13 IC_{50} = 9 nM; Colo205 IC_{50} = 11 nM; >1000-fold selectivity for CDK4 over CDK1; >200-fold cellular off/on targets ratio; pRb IC_{50} = 23 nM and pSTAT5 IC_{50} = 52 nM in MOLM13 cell line, respectively), and we were pleased to find that this molecule exhibited good-to-moderate pharmacokinetics across the three species studied (rat, mouse, and dog). A dose-dependent decrease in Rb phosphorylation (pRb) was observed in a MOLM13 mouse xenograft PD study with **19** starting at the 37.5 mg/kg dose (Figure 4b). In addition, a dose-dependent increase in drug concentration in plasma was observed. However, drug exposures in mouse neither led to a dose-dependent reduction in STAT5 phosphorylation (pSTAT5) nor a sufficient decrease in pSTAT5 even at the 150 mg/kg dose (Figure 4a). This may have been due to limited drug exposure levels in the mouse plasma (unbound C_{max} = 0.024 μ M at 150 mg/kg dose, much lower than cellular IC_{50} of pSTAT5 in MOLM13 of 52 nM).

Reasoning that further optimization of the physicochemical properties would be required for achieving efficacious drug exposures, and knowing that the charged amine group of our inhibitors was associated with reduced phospholipid membrane permeability and intestinal absorption and with increased efflux rates, we next turned our attention toward less basic polar surrogates for the amine moiety of **19**. Representative nonbasic analogues are shown in Figures 5 and 6 and discussed in detail below.

First, we considered that ethanolamine derivatives, exemplified by **22**, might benefit from several advantages, including reductions in basicity compared to **19** (pK_a = 9.2) through either inductive or hydrogen-bonding effects as well as possible stabilization of the ion pairs required for efficient passive diffusion of the protonated structure (Figure 5).¹⁷ Propanolamine **22** indeed gave much higher drug exposure in the rat (total C_{max} = 0.28 μ M and AUC = 3.24 μ M·h at the 2 mg/kg oral dose) than **19** (total C_{max} = 0.13 μ M and AUC = 1.57 μ M·

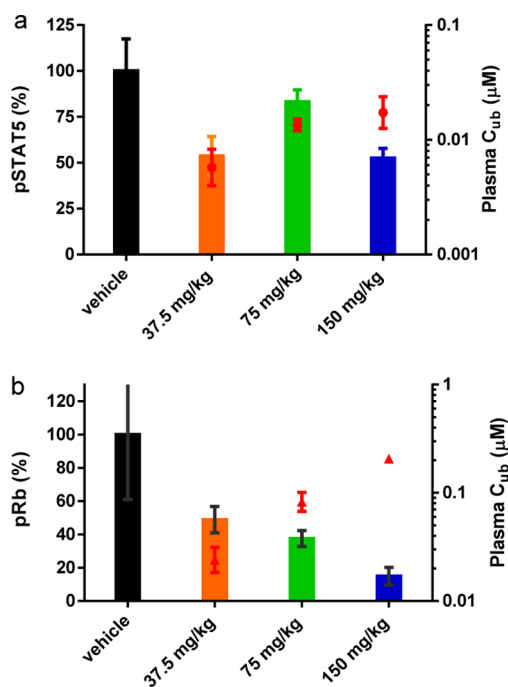


Figure 4. STAT5 and Rb phosphorylation in MOLM13 tumors treated with **19**. MOLM13 tumor bearing mice were dosed by oral administration of **19** at 37.5, 75, or 150 mg/kg, and tumors were harvested at 3 and 24 h after treatment. Tumors lysates were prepared and the level of pSTAT5 (at 3 h post dose, (a)) or pRb (at 24 h post dose, (b)) was determined. Unbound plasma levels of **19** (μ M) at the same time points are shown. Data are presented as mean \pm SEM, n = 3 except for vehicle group (n = 6).

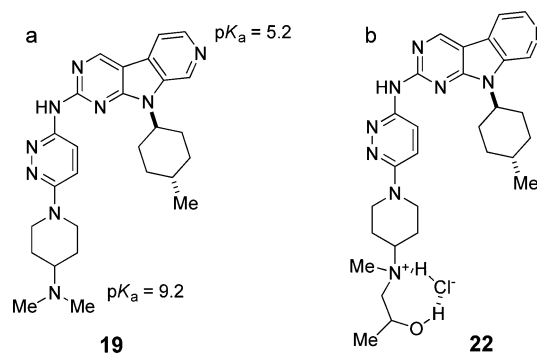


Figure 5. (a) Experimentally measured pK_a of compound **19**; (b) R_4N^+ and Cl^- ion pair may be stabilized by hydrogen bonds.

h at the 2 mg/kg oral dose). Unfortunately, further development of this series was precluded by high binding affinities for hERG (IC_{50} = 0.92 μ M) and moderate-to-high clearance in the dog.

Ultimately, we sought to replace the basic amine with an effectively nonbasic polar surrogate (e.g., **23–28**). Glycolamides, sulfones, and various spiro-lactams all resulted in dramatically improved pharmacokinetic properties, particularly increased drug exposures in high-dose mouse experiments (Figure 6) at the expense of modest reductions in potency (Table 4).

Among these analogues, compound **28** (AMG 925) emerged as the most suitable candidate for clinical development by virtue of its excellent pharmacokinetic properties (in rat, CL = 0.39 L/h/kg, $F\%$ = 75), well-balanced inhibitory activities on

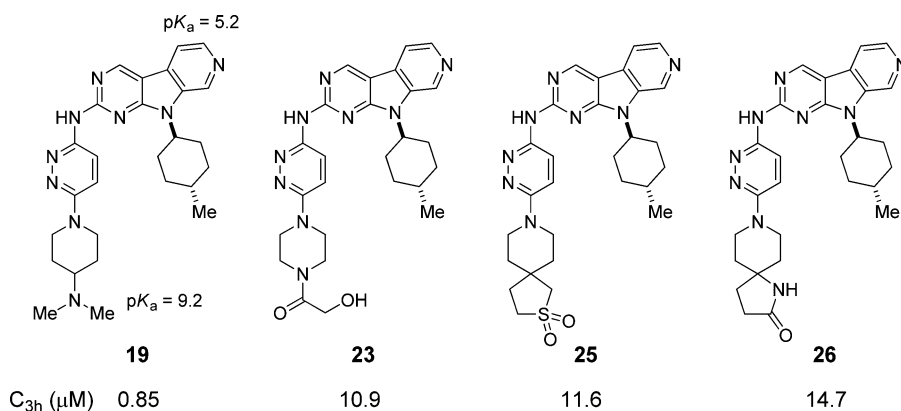


Figure 6. Drug exposure levels vs molecular basicity (C_{3h} : total drug concentration at 3 h post 150 mg/kg oral dose in mouse PK studies).

Table 4. Optimization of the Heteroaryl Linker^a

	22	23	24	25	26	27	28
R							
CDK4/D1 IC ₅₀ (μM)	0.003	0.003	0.009	0.004	0.003	0.013	0.003
FLT3 IC ₅₀ (μM)	0.006	0.008	0.008	0.005	0.003	0.0006	0.001
CDK1/B IC ₅₀ (μM)	1.54	1.05	3.97	1.63	1.77	1.06	2.22
Colo205 IC ₅₀ (μM)	0.009	0.031	0.019	0.038	0.031	0.044	0.055
MOLM13 IC ₅₀ (μM)	0.004	0.037	0.030	0.032	0.021	0.004	0.019
MDA-MB436 IC ₅₀ (μM)	0.91	1.19	10.0	10.0	7.23	7.50	3.83
Rat CL (L/h/kg)	0.60	0.12	0.20	0.54	1.3	0.91	0.39
F (% , rat) ^b	46	22	23	38	48	65	75

^aValues were the means of at least three determinations; standard deviation was $\pm 30\%$. ^bFormulation: 1.5% sodium acetate/pH4.

Table 5. Binding Affinity of **28** to Wild-Type and Mutant FLT3

	FLT3 ^{WT}	FLT3 ^{ITD}	FLT3 ^{D835Y}	FLT3 ^{D835H}	FLT3 ^{K663Q}	FLT3 ^{N841I}
K_d (μM)	0.004	0.004	0.001	0.001	0.004	0.004

FLT3 and CDK4 with good selectivity against the Kinome Scan panel¹⁸ (Supporting Information Tables 1 and 2), potent antiproliferation efficacy against MOLM13 cells, and superior safety profile and in vitro ADME properties (data not shown).

With a suitable candidate now in hand, we evaluated **28** against a panel of activated variants of FLT3. Activating mutations of kinases are commonly observed in cancer and can be selected by treatment with type II inhibitors, promoting the development of cancer that is more difficult to treat and leading to an acute need for agents that efficaciously target these

mutations.⁸ Gratifyingly, **28** exhibited excellent binding affinities (1–4 nM) for all of the FLT3 mutants available in the KINOMEScan (data in Table 5). This high affinity for mutated forms of FLT3, particularly those mutants known to confer pronounced resistance to FLT3-inhibition monotherapy, make compound **28** very attractive for clinical development.

The activity of **28** in various tumor cell lines demonstrated its ability to block FLT3 and CDK4. Compound **28** showed potent and broad antiproliferation activities against AML cell lines independent of the FLT3 mutation status while

maintaining simultaneous inhibition of CDK4. Compound **28** inhibited pSTAT5 in MOLM13 and pRb in Colo205 with IC_{50} s of 0.005 and 0.023 μ M, respectively, indicating that the observed efficacy in vitro was consistent with FLT3 and CDK4 inhibition (Table 6). In contrast, sorafenib,¹⁹ a multikinase

Table 6. The Antiproliferation Activity of **28 in Comparison with a CDK4/6 and FLT3 Inhibitor^a**

	28	palbociclib	sorafenib
FLT3 IC_{50} (μ M)	0.001	3.48	0.004
CDK4 IC_{50} (μ M)	0.003	0.002	>3
pSTAT5 IC_{50} (μ M)	0.005	>3	0.002
pRb IC_{50} (μ M)	0.023	0.011	>3
MOLM13 IC_{50} (μ M)	0.019	0.096	0.005
U937 IC_{50} (μ M)	0.052	0.14	>3
MOLM13 ^{SR} IC_{50} (μ M)	0.023	0.096	>3
Colo205 IC_{50} (μ M)	0.055	0.036	>3

^aThe antiproliferation activity was determined by ¹⁴C-thymidine incorporation DNA synthesis assay; MOLM13^{SR}: (FLT3^{ITD+D835Y}) clone was isolated by culturing MOLM13 in the presence of 1 nM Sorafenib. Resistance cells were isolated in about 6 weeks, and the cells can rapidly adapt to >1 μ M of sorafenib in culture (about 2 weeks from 1 nM to 1 μ M).

inhibitor with FLT3 activity, showed potent inhibitory activity toward the FLT3^{ITD} mutant MOLM13 cell line but almost no activity against U937, a FLT3 wild-type AML cell line. In contrast to palbociclib,¹⁹ a CDK4/6 inhibitor, which arrests Rb positive tumor cells including MOLM13 in G1 stage, **28** induced apoptosis in FLT3^{ITD} AML cell lines and the FLT3^{ITD,D835Y} mutant AML cell line, the latter being a mutant strain cultivated to exhibit marked resistance to sorafenib by continuously treating MOLM13(FLT3^{ITD}) cells with gradually increased concentration of sorafenib (from 1 to 1000 nM) over the course of several weeks (Table 7). Analogous experiments

Table 7. Compound **28 Induced Apoptosis in FLT3 Mutant AML Cells^a**

	28	palbociclib	sorafenib	control
U937 (FLT3 ^{WT})	23.68	9.09	8.76	7.14
MOLM13 (FLT3 ^{ITD})	82.30	16.95	84.60	5.44
MOLM13 ^{SR} (FLT3 ^{ITD+D835Y})	70.86	8.35	5.16	7.57

^aMOLM13, MOLM13SR, and U937 cells were treated with **28**, palbociclib, and sorafenib at 1 μ M for 48 h, individually. The treated cells were stained with Annexin V/Sytox Green and analyzed by flow cytometry for apoptosis. Data represent percentage of apoptotic cells in total cells analyzed.

conducted with the concentration of **28** ranging as high as 10 nM over treatment durations as long as 4 months failed to produce appreciable resistance to **28** (IC_{50} = 0.028 μ M), and sequencing analysis showed that no additional FLT3 mutations had been produced under these conditions.²⁰ These results are consistent with the hypothesis that dual inhibition of FLT3 and CDK4 make it more challenging for AML cells to develop resistance to FLT3 inhibition than in the case of FLT3-inhibition monotherapy. In aggregate, these data indicate that the FLT3/CDK4 dual inhibitor **28** has broader activity, and is potentially more effective in treating AML, than the current therapeutic agents.

To understand the structural properties that result in the differential activities against FLT3 mutants of sorafenib and **28**,

respectively, we modeled the binding modes of the two compounds to FLT3, the conformation of the activation loop (DFG-in, DFG-out),²¹ and key FLT3 activation mutations and how they affect the activation loop conformation. The activation loop in a kinase is inherently flexible and capable of multiple conformations. For this analysis, we focused on two representative conformations, DFG-in as the active conformation and DFG-out as the inactive conformation. Previously published binding data suggest that sorafenib is a type II kinase inhibitor that preferentially binds to the inactive DFG-out kinase conformation.²² In this sorafenib–FLT3 model, the phenolic ring of sorafenib would form a perpendicular aromatic–aromatic interaction with F830 in the DFG motif (Figure 7c), which is one of the key interactions with the

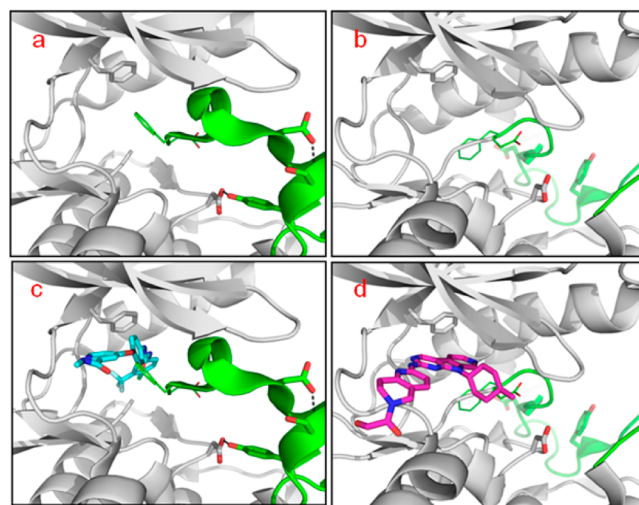


Figure 7. Computational models of binding modes and activation loop conformations of inactive DFG-out and active DFG-in activation loop conformations.^{14,23} (a) DFG-out kinase with the activation loop (green) in the inactive conformation stabilized by intramolecular hydrogen bonds. (b) DFG-in kinase with the activation loop (green) in the active DFG-in conformation. (c) DFG-out kinase with sorafenib model showing type 2 binding mode. (d) DFG-in kinase with **28** model showing type I binding mode.

protein. This interaction would not be possible in the active DFG-in kinase conformation. In this inactive, DFG-out conformation, FLT3 native residues D835 and Y842 stabilize this conformation of the activation loop by forming hydrogen bonds with the main chain amide group S838 and side chain D811, respectively (Figure 7a). Thus, replacement of either residue might destabilize the inactive conformation of the activation loop, which would then be expected to hinder the binding of sorafenib.

In contrast, **28** is a type I kinase inhibitor and preferentially binds to the active DFG-in conformations (Figure 7d) and maintains activity against those activation loop single point mutations.

The pharmacokinetic profiles of **28** were investigated in rat, dog, and cynomolgus monkey (Table 8). Plasma elimination half-lives following intravenous dosing range from 1.7 h in dog to 5.6 h in monkey. Steady state volumes of distribution values (V_{ss}) were fairly constant across species, with values ranging from 1.8 L/kg in rat to 3.8 L/kg in cynomolgus monkey. The plasma clearance in rat was low relative to hepatic blood flow, while it was moderate to high in dog and moderate in cynomolgus monkey. In all species, the compound showed

Table 8. Pharmacokinetic Parameters of 28 in Rat, Dog, and Cynomolgus Monkey

species	CL (L/h/kg)	V _{ss} (L/kg)	T _{1/2,z} (h)	F (%)
rat ^a	0.39	1.8	5.5	75
dog ^{b,c}	1.41	2.6	4.1	ca. 100
monkey ^{b,c}	1.42	3.2	6.6	44

^aVehicle used in iv and po studies in rat: water/acetate/tween at pH4, 96/3/1 (v/v/v). ^bVehicle used in iv studies in dog and monkey: 40% PG aqueous solution at pH2. ^cVehicle used in po studies in dog and monkey: 20% captisol aqueous solution.

moderate to high oral bioavailability following gavage administration in solution formulation. This preclinical pharmacokinetic profile was the basis for predicting, using in vitro–in vivo extrapolation methods, human oral clearance of 0.21 L/h/kg and a terminal phase half-life of 3.3 h, a profile consistent with twice-daily dosing.

The combination of potent tumor cell growth inhibition in vitro and high exposure led to significant antitumor effects in vivo. NCR nude mice bearing MOLM13 tumors were treated with 28 orally at doses of 25, 50, 75, and 150 mg/kg once daily for 8 days. Dose-dependent inhibition of tumor growth was observed with 100% tumor growth inhibition (TGI) at 150 mg/kg dose (Figure 8). The calculated ED₅₀ was 22 mg/kg,

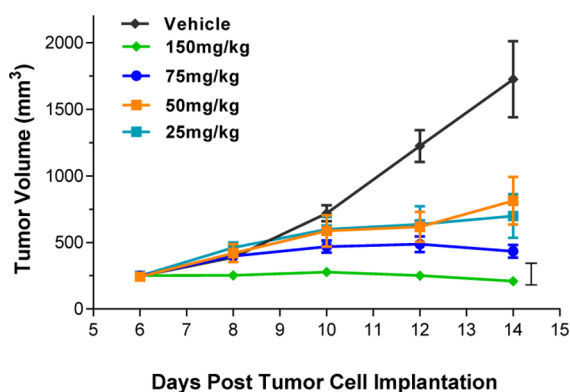


Figure 8. In vivo tumor growth inhibition for 28. NCR nude mice bearing established human MOLM13 AML xenografts were dosed orally with either vehicle or 28 at 25, 50, 75, and 150 mg/kg (day 14 TGI = 100%, $p < 0.0001$) once daily from day 5 to day 13.

and the corresponding AUC was determined to be 28 $\mu\text{M}\cdot\text{h}$ from terminal PK analyzed from plasma harvested after the final dose (Supporting Information Figure 1). Body weight losses were within an acceptable range (10%) throughout the study (Supporting Information Figure 2), and 28 was well tolerated. In addition, the phosphorylation of STAT5, which is an important downstream signaling protein of FLT3 signaling, and the phosphorylation of Rb, a downstream protein of the CDK4 pathway, were also significantly reduced in MOLM13 tumor tissues obtained from the 28 treated group compared with the vehicle group (Figure 9), indicating that the observed efficacy in vivo was consistent with FLT3 and CDK4 signaling inhibition.

SYNTHETIC CHEMISTRY

The general approach to the pyrido[4',3':4,5]pyrrolo[2,3-d]pyrimidine series of dual inhibitors (Figure 10) fashioned the key C–N bonds using nucleophilic aromatic substitution and Hartwig–Buchwald amination sequences and established

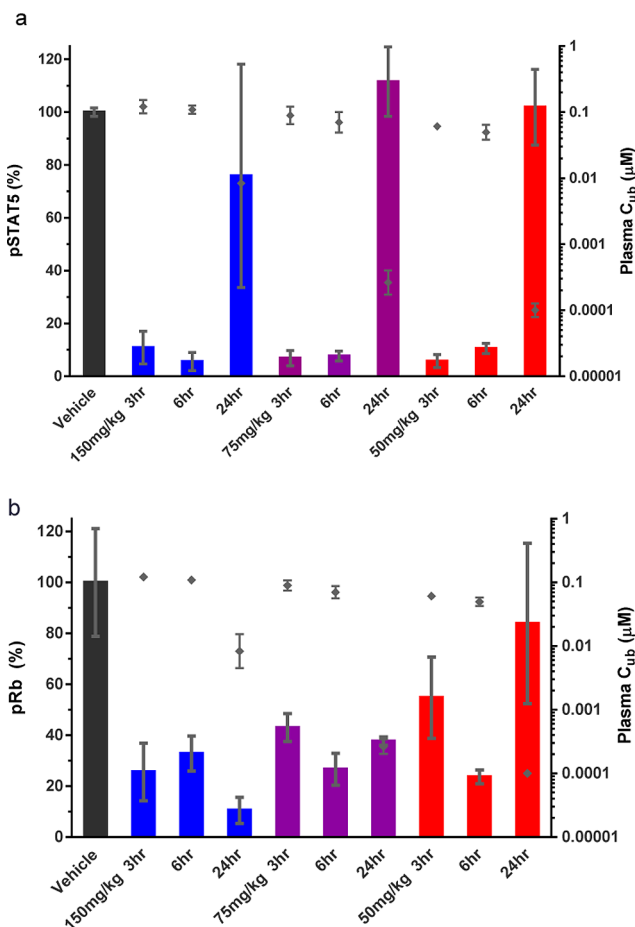


Figure 9. Compound 28 inhibited STAT5 (a) and Rb (b) phosphorylation in MOLM13 subcutaneous tumors. MOLM13 tumor bearing mice were dosed by oral administration of 28 at 50, 75, or 150 mg/kg, and tumors were harvested at 3, 6, and 24 h after treatment. Tumors lysates were prepared, and the level of pSTAT5 (upper panel) or pRb (lower panel) was determined.²⁴ Unbound plasma levels of 28 (μM) same time points are shown. Data are presented as mean \pm SEM, $n = 3$ except for vehicle group ($n = 6$).

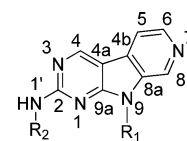
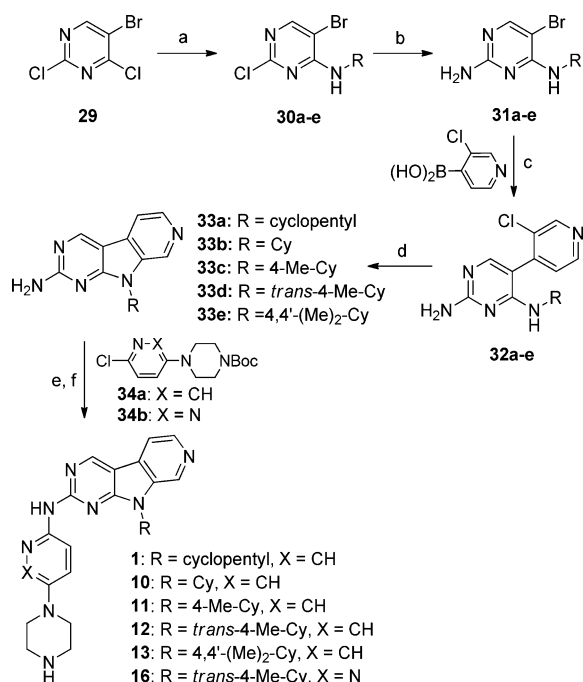


Figure 10. Numbering convention used for the pyrido[4',3':4,5]-pyrrolo[2,3-d]pyrimidine core.²⁶

the C4a–C4b heterobiaryl bond through either Negishi or Suzuki cross-coupling (Scheme 1). Early variants of this strategy generated bromopyrimidine Suzuki substrates 31a–e in a two-step substitution sequence beginning with primary aliphatic amines of interest and commercially available 5-bromo-2,4-dichloropyrimidine 29. Variation of the amine substituent at this juncture enabled broad characterization of SAR trends associated with the cycloalkane sugar-pocket group displayed at N9 of the tricyclic core (Table 2, 8–14).²⁵ The N9–C8a bond establishing the fused pyrrole ring of the core was formed by intramolecular Hartwig–Buchwald amination of heterobiaryl cross-coupling products 32a–e, with subsequent installation of the heteroarene substituent at N1' by intermolecular amination of haloheteroarenes 34. Piperazine

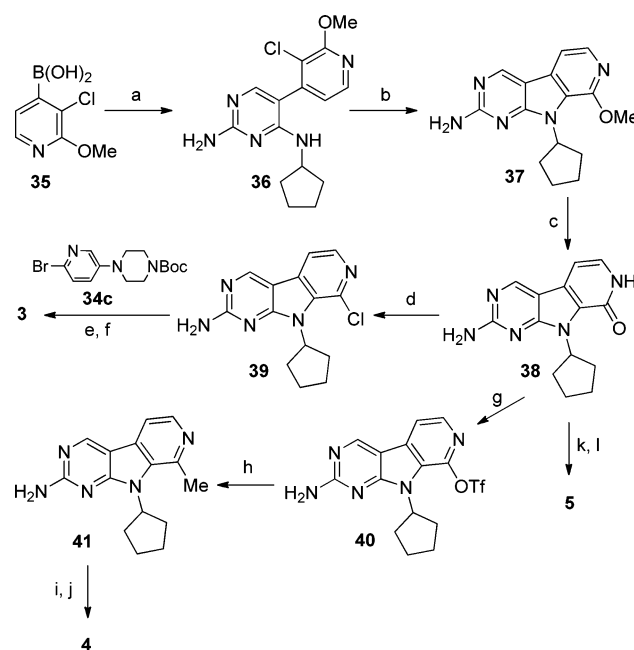
Scheme 1. First-Generation Synthetic Approach to the Pyrido[4',3':4,5]pyrrolo[2,3-d]pyrimidine Dual Inhibitors^a

^aReagents and conditions: (a) RNH₂, DIPEA, reflux; (b) NH₄OH, *i*-PrOH, 120 °C; (c) PdCl₂(PPh₃)₂, Na₂CO₃, 1,4-dioxane, 120–150 °C; (d) Pd₂dba₃, XantPhos, *t*-BuONa, 1,4-dioxane, 150 °C; (e) Pd₂dba₃, XantPhos, *t*-BuONa, 1,4-dioxane, 120 °C; (f) TFA/CH₂Cl₂.

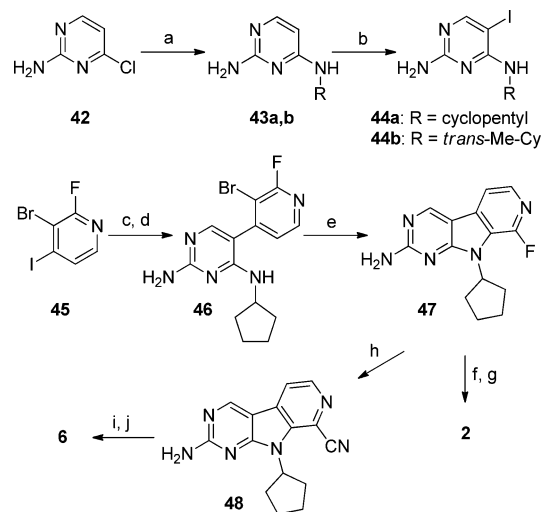
derivatives (e.g., lead compound **1**) were liberated upon acidic cleavage of the *t*-butylcarbamoyl group, and alkylation or acylation of the resulting basic nitrogen function enabled the preparation of an array of higher analogues (e.g., **23**).

Our discovery efforts ultimately led us toward extensive characterization of SAR trends associated with the fused pyridine ring of the tricyclic core, with particular concentration in studying the effects of substitution at C8. We found it most expedient to prepare many of the substituted pyridine analogues via interconversions between pyridone derivatives (Scheme 2). The parent pyridone core **38** could be readily obtained from methoxypyridine **37** and thus from commercially available methoxypyridylboronic acid **35**. Certain analogues more easily accessed when the synthesis design was modified to employ a milder construction of the heterobiaryl C4a–C4b bond by Negishi coupling of iodopyrimidines **44a,b** (Scheme 3) with suitable arylzinc precursors. *ortho*-Fluoropyridine **2** could thus be prepared by directed lithiation/transmetalation of iodobromofluoropyridine **45** (Scheme 3). *ortho*-Cyano derivatives (e.g., **6**) were in turn generated from a common fluoropyridine intermediate **47** by the action of tetraethylammonium cyanide in hot DMF (Scheme 3). Synthesis of pyridazine derivative **7** also proceeded by way of Negishi chemistry (Scheme 4), with formation of the central ring via nucleophilic displacement.

Surveying the effects of varying the cycloalkane and fused-pyridine binding motifs led to identification of **33d** as the optimal scaffold, and our escalating demand for this material necessitated the development of a highly efficient and scalable route from cost-effective precursors. Applying the Negishi methodology developed above, we were gratified to discover that the readily available feedstock 3-fluoropyridine **54**

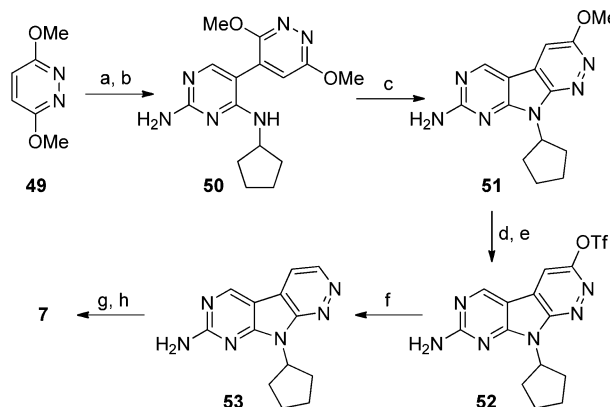
Scheme 2. Synthesis of *ortho*-Substituted Pyridine Analogues via Pyridone **38**^a

^aReagents and conditions: (a) **31a**, PdCl₂(PPh₃)₂, Na₂CO₃, 1,4-dioxane, 120 °C; (b) Pd₂dba₃, XantPhos, *t*-BuONa, 1,4-dioxane, 150 °C; (c) HCl, 1,4-dioxane/MeOH, 80 °C; (d) POCl₃, 100 °C; (e) Pd₂dba₃, XantPhos, *t*-BuONa, 1,4-dioxane, 80 °C; (f) TFA/CH₂Cl₂; (g) Tf₂NPh, NaH, DMF; (h) Fe(acac)₃, MeMgBr, THF/NMP; (i) **34a**, Pd₂dba₃, XantPhos, *t*-BuONa, 1,4-dioxane, 120 °C; (j) TFA/CH₂Cl₂; (k) **34a**, Pd₂dba₃, XantPhos, *t*-BuONa, 1,4-dioxane, 120 °C; (l) TFA/CH₂Cl₂.

Scheme 3. Negishi Coupling Approach to Substituted Fused Pyridine Derivatives **2** and **6**^a

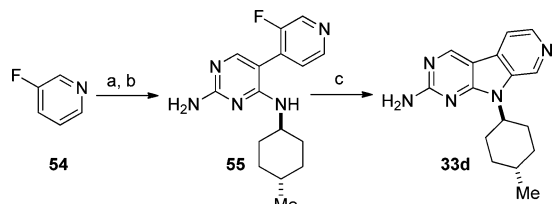
^aReagent and conditions: (a) cyclopentylamine or *trans*-Me-cyclohexylamine, 1,4-dioxane or BuOH, 100 °C; (b) NIS, DMF or AcOH, 80 °C; (c) *i*-PrMgCl, ZnCl₂; (d) **44a**, Pd(PPh₃)₄, THF, reflux; (e) X-phos, Cs₂CO₃, 1,4-dioxane, 120 °C; (f) **34a**, Pd₂dba₃, XantPhos, *t*-BuONa, 1,4-dioxane, 120 °C; (g) TFA/CH₂Cl₂; (h) NEt₄CN, DMF, 150 °C; (i) **34a**, Pd₂dba₃, XantPhos, *t*-BuONa, 1,4-dioxane, 120 °C; (j) TFA/CH₂Cl₂.

underwent high-yielding and facile cross-coupling with **44b** upon directed lithiation by LiTMP at cryogenic temperature

Scheme 4. Negishi Route to Fused Pyridazine Derivative 7^a

^aReagents and conditions: (a) LiTMP, ZnCl₂; (b) **44a**, Pd(PPh₃)₄, THF, reflux; (c) NaH, THF, 150 °C; (d) PPTS, 180 °C; (e) PhNTf₂, TEA, DMAP; (f) Pd(OAc)₂, dppf, TEA, HCO₂H, DMF; (g) **34a**, Pd₂dba₃, XantPhos, *t*-BuONa, 1,4-dioxane, 120 °C; (h) TFA/CH₂Cl₂.

followed by transmetalation to zinc bromide (Scheme 5).^{27,28} Intramolecular displacement of fluoride by the pendant

Scheme 5. Process Synthesis of Optimized Tricyclic Core **33d**^a

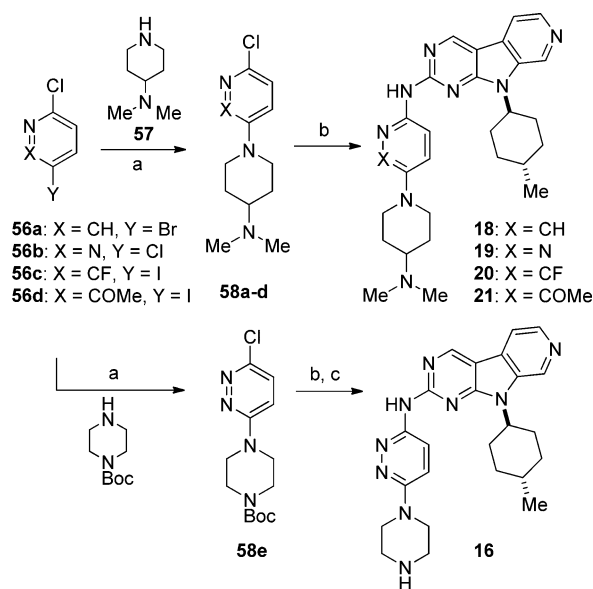
^aReagents and conditions: (a) LiTMP, ZnBr₂, -78 °C; (b) **44b**, Pd(PPh₃)₄, THF, reflux; (c) LiHMDS, NMP, 90 °C.

secondary amine function in the presence of LiHMDS completed the synthesis of **33d**. The optimized sequence enabled rapid preparation of kilogram quantities of this critical intermediate.

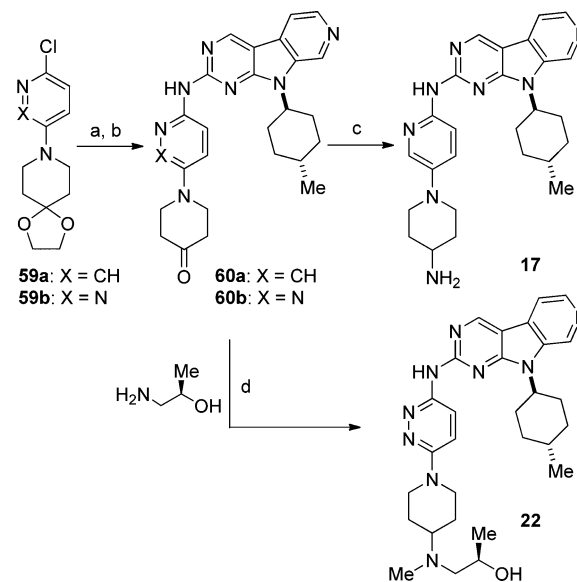
Exploring SAR trends associated with the N1' pyridyl substituent and the piperazine ring (more generally, the distal solubilizing group) situated at its 5 position required us to prepare a wide array of haloheteroarene Hartwig–Buchwald substrates (**58a–d**, Scheme 6); this was generally accomplished by arylating the corresponding secondary amines (e.g., **57**). Studies directed at optimizing substituents on the basic nitrogen in the 4-aminopiperidine series effected late-stage diversification by reductive amination of advanced ketones **60a,b** (illustrated for **17** and **22**, Scheme 7).

Derivatives featuring nonbasic distal solubilizing moieties often required the development of more involved, target-specific methodologies. Syntheses of representative compounds from the most important classes are outlined in Schemes 8–10. The halopyridazine precursor **64** to aliphatic sulfone **24** was prepared from primary alcohol **61** by a straightforward amination/mesylation/SN₂ methylsulfonation/oxidation sequence (Scheme 8).

Arylation of the spirocyclic piperidines **65** and **68** gave the corresponding amidation substrates **66**, **69a**, and **69b** used to prepare compounds **25–27** (Scheme 9).

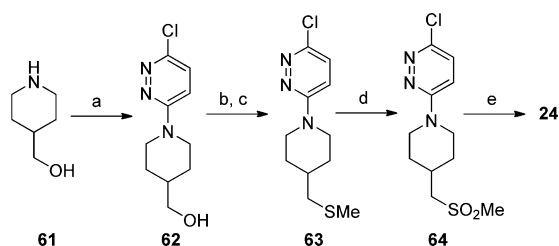
Scheme 6. Synthesis and Coupling of Haloheteroarene Amination Substrates^a

^aReagents and conditions: (a) Pd₂dba₃, XantPhos, *t*-BuONa or Cs₂CO₃, 1,4-dioxane or PhMe, 90–120 °C (for **58a**, **58c–d**), DIPEA, 1,4-dioxane, 80 °C (for **58b,e**); (b) **33d**, Pd₂dba₃, XantPhos, *t*-BuONa or Cs₂CO₃, 1,4-dioxane or PhMe, 100–120 °C; (c) TFA/CH₂Cl₂.

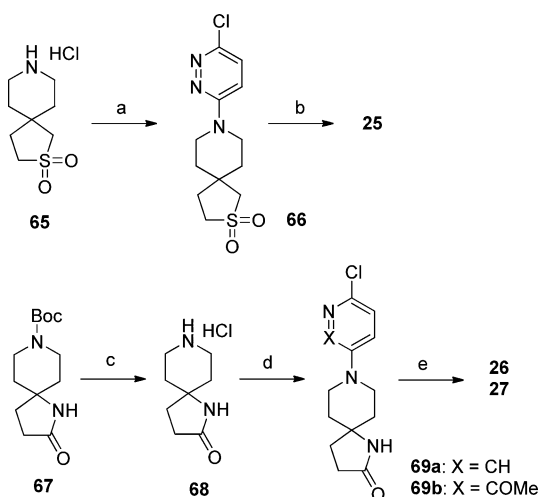
Scheme 7. Modular Approach to 4-Aminopiperidine Derivatives **17** and **22** via Late-Stage Reductive Amination^a

^aReagents and conditions: (a) **33d**, Pd₂dba₃, XantPhos, *t*-BuONa, 1,4-dioxane; (b) 6N HCl (aq); (c) NaBH₃(CN), NH₄OAc, MeOH, 60 °C; (d) NaBH(OAc)₃, H₂CO (aq), CH₂Cl₂.

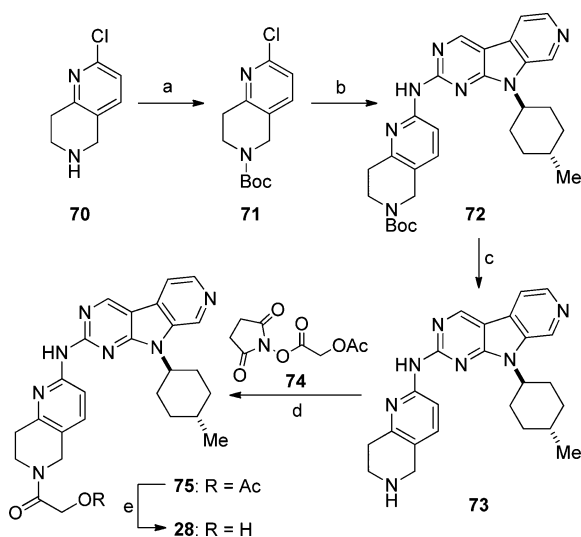
Finally, the requisite amination substrate for the synthesis of **28** could be prepared by Boc protection of commercially available chlorotetrahydronaphthyridine **70** (Scheme 10). Hartwig–Buchwald coupling of **71** with **33d** and subsequent Boc deprotection both occurred in virtually quantitative yields under optimized conditions. Acetoxyacetylation and acetate saponification completed the synthesis, giving **28** in high overall yield (97% from **70**).

Scheme 8. Synthesis of the Precursor to Aliphatic Sulfone 24^a

^aReagents and conditions: (a) **56b**, 90 °C; (b) MsCl, TEA; (c) NaSMe, DMF; (d) oxone, MeOH; (e) **33d**, Pd₂dba₃, XantPhos, *t*-BuONa, 1,4-dioxane, 120 °C.

Scheme 9. Synthesis of the Precursor to Spirocyclic Sulfone and Spirocyclic Lactams^a

^aReagents and conditions: (a) **56b**, DIPEA, 1,4-dioxane, 90 °C; (b) **33d**, Pd₂dba₃, XantPhos, *t*-BuONa, 1,4-dioxane, 150 °C; (c) HCl, 1,4-dioxane; (d) **56a** or **56d**, XantPhos, Pd₂dba₃, *t*-BuONa, PhMe; (e) **33d**, Pd₂dba₃, XantPhos, *t*-BuONa, 1,4-dioxane, 150 °C.

Scheme 10. Synthesis of **28**^a

^aReagents and conditions: (a) (Boc)₂O, DIPEA, DCM; (b) **33d**, Pd₂dba₃, XantPhos, *t*-BuONa, 1,4-dioxane, 100 °C; (c) HCl, MeOH/H₂O; NaOH; (d) DIPEA, CHCl₃; (e) MeONa, DCM/MeOH.

CONCLUSION

From lead compound **1**, a combination of structure-based drug design, traditional, and novel medicinal chemistry approaches led to the discovery of **28**, a FLT3/CDK4 dual inhibitor with preferential affinity for the activated state of FLT3. Compound **28** shows potent in vitro activities against CDK4 and FLT3, including several key FLT3 mutants, and displays potent antitumor efficacy mediated by inhibition of FLT3 and Rb phosphorylation in vivo. Compound **28** possesses excellent cross-species pharmacokinetic properties in multiple preclinical models. Compound **28** may improve the durability of clinical response in the treatment of AML by simultaneously modulating two key targets.

EXPERIMENTAL SECTION

General Chemistry. All reactions were conducted under an inert gas atmosphere (nitrogen or argon) using a Teflon-coated magnetic stirbar at the temperature indicated. Commercial reagents and anhydrous solvents were used without further purification. Removal of solvents was conducted by using a rotary evaporator, and residual solvent was removed from nonvolatile compounds using a vacuum manifold maintained at approximately 1 Torr. All yields reported are isolated yields. Preparative reversed-phase high pressure liquid chromatography (RP-HPLC) was performed using an Agilent 1100 series HPLC and Phenomenex Gemini C18 column (5 μm, 100 mm × 30 mm i.d.), eluting with a binary solvent system A and B using a gradient elution [A, H₂O with 0.1% trifluoroacetic acid (TFA); B, CH₃CN with 0.1% TFA] with UV detection at 220 nm. All bioassayed compounds were purified to ≥95% purity as determined by a Agilent 1100 series HPLC with UV detection at 220 nm using the following method: Zorbax SB-C8 column (3.5 μm, 150 mm × 4.6 mm i.d.); mobile phase, A = H₂O with 0.1% TFA, B = CH₃CN with 0.1% TFA; gradient, 5–95% B (0.0–15.0 min); flow rate, 1.5 mL/min. Low-resolution mass spectral (MS) data were determined on an Agilent 1100 series LCMS with UV detection at 254 nm and a low-resolution electrospray mode (ESI). High-resolution mass spectra (HRMS) were obtained on an Agilent 6510 Q-TOF MS with an Agilent 1200 LC on the front end. ¹H NMR spectra were obtained on a Bruker Avance III 500 (500 MHz) or Bruker Avance II 400 (400 MHz) spectrometer. Chemical shifts (δ) are reported in parts per million (ppm) relative to residual undeuterated solvent as an internal reference. The following abbreviations were used to explain the multiplicities: s = single, d = doublet, t = triplet, q = quartet, dd = doublet of doublets, dt = doublet of triplets, m = multiplet, br = broad.

5-Bromo-2-chloro-N-cyclopentylpyrimidin-4-amine (30a). To a solution of 5-bromo-2,4-dichloropyrimidine (45.6 g, 200 mmol) in dioxane (400 mL) was added *N*-cyclopentylamine (20.4 g, 240 mmol) at room temperature. The mixture thus obtained was stirred at room temperature for 6 h. The reaction mixture was then diluted with ethyl acetate, washed with brine, and dried over MgSO₄. The solvent was evaporated to give compound **30a** as light-yellow solid (56 g, 100% yield). ¹H NMR (500 MHz, DMSO-*d*₆) δ ppm 8.23 (1H, s), 7.37 (1H, d, *J* = 7.3 Hz), 4.31 (1H, m), 1.92 (2H, m), 1.71 (2H, m), 1.53–1.59 (4H, m). MS (ESI) *m/z*: 276.0 [M + H]⁺.

5-Bromo-N⁴-cyclopentylpyrimidine-2,4-diamine (31a). A solution of **30a** (45 g, 200 mmol) in 28% NH₄OH/2-propanol (1/1, 400 mL) was heated at 120 °C in sealed tube for 22 h. The product was extracted with dichloromethane, and the organic layers were washed with brine and dried. The solvent was evaporated, and the residue was purified by flash chromatography on silica gel eluting with 25% ethyl acetate in hexanes to give compound **31a** as white solid (34 g, 66% yield). ¹H NMR (500 MHz, DMSO-*d*₆) δ ppm 7.77 (1H, s), 6.19 (2H, br s), 6.12 (1H, d, *J* = 7.3 Hz), 4.33 (1H, m), 1.90 (2H, m), 1.69 (2H, m), 1.49–1.55 (4H, m). MS (ESI) *m/z*: 257.0 [M + H]⁺.

5-(3-Chloropyridin-4-yl)-N⁴-cyclopentylpyrimidine-2,4-diamine (32a). To a solution of **31a** (2.57 g, 10.0 mmol) in dioxane (75 mL) were added 3-chloropyridine-4-boronic acid (4.72 g, 10.0 mmol),

$\text{PdCl}_2(\text{PPh}_3)_2$ (702 mg, 1.0 mmol), and sodium carbonate (3.82 g, 36 mmol, in 36 mL of water). The mixture thus obtained was purged with N_2 for 10 min and heated at 120 °C in a sealed tube for 22 h. The reaction mixture was diluted with water, and the product was extracted with chloroform. The organic layers were dried over MgSO_4 and concentrated. The residue was purified by flash chromatography on silica gel, eluting with 2.5% methanol in dichloromethane to give compound **32a** as white solid (2.31 g, 80% yield). $^1\text{H NMR}$ (500 MHz, $\text{DMSO}-d_6$) δ ppm 8.64 (1 H, s), 8.50 (1 H, d, $J = 4.9$ Hz), 7.51 (1 H, s), 7.34 (1 H, d, $J = 4.9$ Hz), 6.21 (2 H, br s), 5.97 (1 H, d, $J = 7.4$ Hz), 4.43 (1 H, p, $J = 7.4$ Hz), 1.84 (2 H, m), 1.62 (2 H, m), 1.40–1.49 (4 H, m). MS (ESI) m/z : 290.0 $[\text{M} + \text{H}]^+$.

9-Cyclopentyl-9H-pyrido[4',3':4,5]pyrrolo[2,3-d]pyrimidin-2-amine (33a). To a solution of **32a** (2.3 g, 7.9 mmol) in 1,4-dioxane (60 mL) were added Pd_2dba_3 (368 mg, 0.4 mmol), XantPhos (696 mg, 1.2 mmol), and sodium *t*-butoxide (1.15 g, 12 mmol). The mixture thus obtained was heated at 150 °C under microwave irradiation for 3 h. The reaction mixture was passed through a short pack silica gel column and concentrated. The residue was purified by flash chromatography on silica gel eluting with 2% methanol in dichloromethane to give compound **33a** as white solid (1.71 g, 85% yield). $^1\text{H NMR}$ (500 MHz, $\text{DMSO}-d_6$) δ ppm 9.05 (1 H, s), 8.87 (1 H, br s), 8.37 (1 H, d, $J = 4.9$ Hz), 7.93 (1 H, d, $J = 5.1$ Hz), 6.97 (2 H, br s), 5.33 (1 H, quin, $J = 8.6$ Hz), 2.27 (2 H, m), 2.04 (4 H, m), 1.76 (2 H, m). HRMS (ESI) m/z : calculated for $[\text{M} + \text{H}]^+$ 254.1400, found 254.1406.

4-(4-Chloro-pyrid-2-yl)-piperidine-1-carboxylic Acid *t*-Butyl Ester (34a). To a solution of 5-bromo-2-chloropyridine (11.54 g, 60 mmol) in toluene (300 mL) were added *t*-butyl 1-piperazinecarboxylate (11.18 g, 60 mmol), sodium *t*-butoxide (8.64 g, 90 mmol), $\text{Pd}_2(\text{dba})_3$ (1.10 g, 1.20 mmol), and XantPhos (2.08 g, 3.6 mmol). The mixture was evacuated and purged with argon (3 cycles), then heated at 100 °C for 5 h. After the reaction went to completion, the mixture was cooled to room temperature, diluted with ethyl acetate (1200 mL), and washed with water (300 mL). The organic solution was concentrated under pressure, and the residue was purified by flash chromatography on silica gel eluting with 17% ethyl acetate in hexane to give compound **34a** as a light-yellow solid (14.6 g, 82% yield). $^1\text{H NMR}$ (400 MHz, CDCl_3) δ ppm 8.02 (1 H, s), 7.19–7.18 (2 H, m), 3.59 (4 H, dd, $J = 12$ Hz, $J = 4$ Hz), 3.14 (4 H, dd, $J = 12$ Hz, $J = 4$ Hz), 1.49 (9 H, s). MS (ESI) m/z : 298.1 $[\text{M} + \text{H}]^+$.

9-Cyclopentyl-N-(5-(1-piperazinyl)-2-pyridinyl)-9H-pyrido[4',3':4,5]pyrrolo[2,3-d]pyrimidin-2-amine (1). To a solution of **33a** (1.6 g, 6.3 mmol) in dioxane (60 mL) were added **34a** (2.3 g, 7.6 mmol), Pd_2dba_3 (293 mg, 0.32 mmol), XantPhos (370 mg, 0.64 mmol), and sodium *t*-butoxide (908 mg, 9.45 mmol). The mixture thus obtained was heated at 150 °C under microwave irradiation for 1 h. The reaction mixture was passed through a short pack silica gel column and concentrated to give *t*-butyl 4-(6-((9-cyclopentyl-9H-pyrido[4',3':4,5]pyrrolo[2,3-d]pyrimidin-2-yl)amino)-3-pyridinyl)-1-piperazinecarboxylate as a yellow solid (3.28 g), which was then treated with TFA/DCM (60 mL, 1:1) at room temperature for 30 min. The reaction mixture was concentrated, and the residue was purified by chromatography on silica gel eluting with $\text{CH}_2\text{Cl}_2/\text{MeOH}/\text{NH}_4\text{OH}$ (200:10:1) to give compound **(1)** as an off-white solid (2.60 g, 98% yield). $^1\text{H NMR}$ (400 MHz, $\text{DMSO}-d_6$) δ ppm 9.86 (1 H, s), 9.28 (1 H, s), 9.01 (1 H, s), 8.68 (1 H, br s), 8.45 (1 H, d, $J = 4$ Hz), 8.23 (1 H, d, $J = 8$ Hz), 8.10 (1 H, d, $J = 4$ Hz), 8.04 (1 H, d, $J = 8$ Hz), 7.54 (1 H, dd, $J = 8$ Hz, $J = 4$ Hz), 5.43 (1 H, quin, $J = 8$ Hz), 3.35 (4 H, m), 3.26 (4 H, m), 2.40 (2 H, m), 2.03–2.10 (4 H, m), 1.78 (2 H, m). HRMS (ESI) m/z : calculated for $[\text{M} + \text{H}]^+$ 415.2354, found 415.2350.

***N*⁴-Cyclopentyl-5-iodo-2,4-pyrimidinediamine (44a).** To a stirred solution of compound **43a** (25.5 g, 143 mmol) in DMF (120 mL) was added *N*-iodosuccinimide (32 g, 143 mmol) in two portions at rt. The resulting mixture was stirred at rt for 2 h. Upon workup, the mixture was poured into a mixture of ice and saturated aqueous sodium carbonate with some sodium sulfite, then extracted with ethyl acetate (2 \times). The combined organics were washed with saturated aqueous sodium carbonate (3 \times), dried over sodium sulfate, and concentrated

in vacuo. The residue was subjected to flash column chromatography on silica gel eluting with 1% methanol in DCM to give compound **44a** as a light-yellow solid (39 g, 73% yield). $^1\text{H NMR}$ (500 MHz, $\text{DMSO}-d_6$) δ ppm 7.89 (1 H, s), 6.18 (2 H, s), 5.63 (1 H, d, $J = 7.6$ Hz), 4.30 (1 H, p, $J = 7.4$ Hz), 1.84–1.96 (2 H, m), 1.61–1.74 (2 H, m), 1.42–1.58 (4 H, m). MS (ESI) m/z : 305.0 $[\text{M} + \text{H}]^+$.

5-Iodo-*N*⁴-((1*r*,4*r*)-4-methylcyclohexyl)pyridine-2,4-diamine (44b). 4-Chloropyrimidine-2-amine (1000 g, 7.72 mol, 1.0 equiv), *trans*-4-methylcyclohexylamine hydrochloride (1500 g, 10.03 mol, 1.3 equiv) and TEA (3.23 L, 23.2 mol, 3.0 equiv) were mixed together in *n*-butanol (8 L). The reaction mixture was heated at reflux for 36 h and monitored using LCMS. Upon completion, the reaction mixture was cooled to room temperature, diluted with water (8 L), and extracted with ethyl acetate (2 \times 10 L). The organic layers were combined, dried over Na_2SO_4 , and concentrated under reduced pressure to give *N*⁴-((1*r*,4*r*)-4-methylcyclohexyl)pyridine-2,4-diamine (**43b**) (1770 g), which was used in the next step without further purification. Compound **43b** (1770 g, 8.58 mol, 1.0 equiv) was dissolved in anhydrous DMF (8 L). To this solution under N_2 atmosphere at 10 °C was added iodosuccinimide (1.93 g, 8.58 mol, 1.0 equiv) in portions over 10 min. Upon completion of the addition, the reaction mixture was stirred at room temperature for 2 h. The reaction was monitored using LCMS. Upon completion, the reaction mixture was cooled using an ice bath, quenched with saturated aqueous sodium carbonate (5 L), and extracted with ethyl acetate (2 \times 15 L). The combined organic extracts were washed with saturated aqueous sodium carbonate (2 \times 5 L), water (3 \times 2 L), dried over Na_2SO_4 , and concentrated under reduced pressure. The residue was purified using column chromatography on silica gel eluting with 25–40% ethyl acetate in hexanes to provide compound **44b** (1470 g, 57% over two steps). $^1\text{H NMR}$ (400 MHz, $\text{DMSO}-d_6$) δ ppm 7.86 (1H, s), 6.16 (2H, br s), 5.48 (1H, d, $J = 8.1$ Hz), 3.85 (1H, m), 1.78 (2H, d, $J = 12.3$ Hz), 1.66 (2H, d, $J = 12.3$ Hz), 1.41–1.27 (3H, m), 0.98 (1H, dd, $J = 12.9, 2.7$ Hz), 0.85 (3H, d, $J = 7.2$ Hz). MS m/z : 333.0 $[\text{M} + \text{H}]^+$.

5-(3-Bromo-2-fluoro-4-pyridinyl)-*N*⁴-cyclopentyl-2,4-pyrimidinediamine (46). In a dry 3 neck 2 L flask equipped with a dry addition funnel, thermometer, and stir bar was added 3-bromo-2-fluoro-4-iodopyridine (83.4 g, 276 mmol) followed by 300 mL of anhydrous THF under an atmosphere of nitrogen. The solution was cooled to –70 °C in a 2-propanol/dry ice bath. A solution of isopropylmagnesium chloride 2.0 M in diethyl ether (145 mL, 290 mmol) was added dropwise over a period of 30 min. The solution was then stirred for 30 min before zinc(II) chloride (0.5 M in THF, 276 mL, 138 mmol) was cannulated in. The solution was warmed to room temperature and stirred for 1 h. The addition funnel was replaced with a reflux condenser and **44a** (28.00 g, 92.1 mmol) was added, followed by $\text{Pd}(\text{PPh}_3)_4$ (5.32 g, 4.60 mmol). The solution was heated overnight at a gentle reflux. After concentrating the solution to 1/10th of the volume under vacuum, it was cooled in an ice bath. To this was added 100 mL of cold saturated NH_4Cl , followed by 500 mL of water. Then 500 mL of 12% 2-propanol/DCM was then added and the solution was stirred at room temperature for 1 h before being filtered through filter paper. The filter cake was washed in succession with water, DCM, and 12% 2-propanol/DCM. The filtrate was partitioned in a separation funnel, and the aqueous layer was washed with 12% 2-propanol/DCM. The organics were dried over MgSO_4 and then concentrated under vacuum. The residue obtained was partially dissolved in DCM then sonicated and filtered to give compound **46** (26.5 g, 82% yield) as a light-yellow solid. $^1\text{H NMR}$ (500 MHz, $\text{DMSO}-d_6$) δ ppm 8.18 (1 H, d, $J = 4.9$ Hz), 7.52 (1 H, s), 7.26 (1 H, dd, $J = 4.9, 0.7$ Hz), 6.34 (2 H, s), 6.12 (1 H, d, $J = 7.6$ Hz), 4.42 (1 H, p, $J = 7.4$ Hz), 1.76–1.96 (2 H, m), 1.55–1.68 (2 H, m), 1.31–1.53 (4 H, m). MS (ESI) m/z : 352.0 $[\text{M} + \text{H}]^+$.

9-Cyclopentyl-8-fluoro-9H-pyrido[4',3':4,5]pyrrolo[2,3-d]pyrimidin-2-amine (47). Compound **46** (0.143 g, 0.41 mmol), and cesium carbonate (0.40 g, 1.2 mmol) were combined in anhydrous 1,4-dioxane (5 mL). Nitrogen was briefly bubbled through the solution before adding $\text{Pd}_2(\text{dba})_3$ (0.037 g, 0.041 mmol) and XantPhos (0.047 g, 0.081 mmol). The solution was heated at 120 °C under microwave irradiation for 1 h. The solution was purified with flash column

chromatography on silica gel eluting with DCM/MeOH/NH₄OH (200:10:1) to give compound **47** (94 mg, 85% yield) as a light-brownish solid. ¹H NMR (500 MHz, DMSO-*d*₆) δ ppm 9.10 (1 H, s), 7.94 (1 H, dd, *J* = 5.2, 1.5 Hz), 7.91 (1 H, dd, *J* = 5.1, 2.9 Hz), 7.10 (2 H, br s), 5.38–5.49 (1 H, m), 2.10–2.23 (2 H, m), 1.93–2.08 (4 H, m), 1.64–1.79 (2 H, m). MS (ESI) *m/z*: 272.0 [M + H]⁺.

9-Cyclopentyl-8-fluoro-N-(5-(1-piperazinyl)-2-pyridinyl)-9H-pyrido[4',3':4,5]pyrrolo[2,3-d]pyrimidin-2-amine (2). Compound **2** was prepared from **47** using chemistry similar to that described in the synthesis of **1**. ¹H NMR (500 MHz, CD₃OD) δ ppm 9.46 (1 H, s), 8.10–8.15 (3 H, m), 8.05 (1 H, d, *J* = 2.9 Hz), 7.64 (1 H, d, *J* = 9.5 Hz), 5.20 (1 H, m), 3.51–3.57 (4 H, m), 3.42–3.51 (4 H, m), 2.40–2.50 (2 H, m), 2.10–2.25 (4 H, m), 1.80–1.90 (2H, m). HRMS (ESI) *m/z*: calculated for [M + H]⁺ 433.2260, found 433.2258.

8-Chloro-9-cyclopentyl-9H-pyrido[4',3':4,5]pyrrolo[2,3-d]pyrimidin-2-amine (39). Compound **39** was prepared from 2-chloro-3-fluoropyridine using chemistry similar to that described in the synthesis of **47**. ¹H NMR (500 MHz, DMSO-*d*₆) δ ppm 9.11 (1 H, s), 8.14 (1 H, d, *J* = 4.9 Hz), 7.98 (1 H, d, *J* = 4.9 Hz), 7.07 (2 H, br s), 5.90 (1 H, quin, *J* = 8.7 Hz), 2.44–2.49 (2 H, m), 2.04–2.13 (2 H, m), 1.95–2.03 (2 H, m), 1.63–1.73 (2 H, m). MS (ESI) *m/z*: 288.1 [M + H]⁺.

8-Chloro-9-cyclopentyl-N-(5-(1-piperazinyl)-2-pyridinyl)-9H-pyrido[4',3':4,5]pyrrolo[2,3-d]pyrimidin-2-amine (3). Compound **3** was prepared using chemistry similar to that described in the synthesis of **1**. ¹H NMR (500 MHz, DMSO-*d*₆) δ ppm 10.56 (1 H, br s), 9.42 (1 H, s), 8.87 (2 H, br s), 8.28 (1 H, d, *J* = 4.9 Hz), 8.19 (1 H, d, *J* = 5.1 Hz), 8.09 (1 H, d, *J* = 2.9 Hz), 7.97 (1 H, d, *J* = 9.0 Hz), 7.75 (1 H, dd, *J* = 9.3, 2.0 Hz), 5.96–6.07 (2 H, m, *J* = 9.2, 8.9, 8.8, 8.8 Hz), 3.37–3.43 (4 H, m), 3.26–3.33 (4 H, m), 2.54–2.65 (2 H, m), 2.01–2.12 (4 H, m), 1.66–1.77 (2 H, m). HRMS (ESI) *m/z*: calculated for [M + H]⁺ 449.1963, found 449.1963.

9-Cyclopentyl-8-methoxy-9H-pyrido[4',3':4,5]pyrrolo[2,3-d]pyrimidin-2-amine (37). Compound **37** was prepared from (3-chloro-2-methoxy-pyridin-4-yl)boronic acid using chemistry similar to that described in the synthesis of **33a**. ¹H NMR (400 MHz, CDCl₃) δ ppm 8.87 (1 H, s), 7.98 (1 H, d, *J* = 5.3 Hz), 7.42 (1 H, d, *J* = 5.3 Hz), 5.70 (1 H, t, *J* = 9.0 Hz), 5.21 (2 H, br s), 4.13 (3 H, s), 2.33–2.47 (2 H, m), 1.98–2.15 (4 H, m), 1.67–1.83 (2 H, m). MS (ESI) *m/z*: 284.0 [M + H]⁺.

2-Amino-9-cyclopentyl-7,9-dihydro-8H-pyrido[4',3':4,5]pyrrolo[2,3-d]pyrimidin-8-one (38). A solution of compound **37** (1.42 g, 5.0 mmol) was dissolved in conc HCl (10.4 mL, 125 mmol), and the solution thus obtained was heated at 140 °C under microwave irradiation for 1 h. The reaction mixture was neutralized to pH 7–8 by addition of sodium carbonate, and the precipitate was collected by filtration, washed with water, and dried under high vacuum to give **38** as a yellow solid (1.35 g, 100% yield) that was used in the next step without further purification. ¹H NMR (400 MHz, DMSO-*d*₆) δ ppm 11.38 (1 H, br s), 8.95 (1 H, s), 7.14 (1 H, d, *J* = 8.0 Hz), 6.87 (1 H, d, *J* = 8.0 Hz), 6.75 (2 H, br s), 5.92 (1 H, quin, *J* = 9.0 Hz), 2.32–2.42 (2 H, m), 1.80–2.07 (4 H, m), 1.54–1.70 (2 H, m). MS (ESI) *m/z*: 270.1 [M + H]⁺.

9-Cyclopentyl-2-((5-(1-piperazinyl)-2-pyridinyl)amino)-7,9-dihydro-8H-pyrido[4',3':4,5]pyrrolo[2,3-d]pyrimidin-8-one (5). Compound **5** was prepared from **38** using the methods described in the synthesis of **1**. ¹H NMR (500 MHz, CD₃OD) δ ppm 9.31 (1 H, s), 8.03 (1 H, s), 8.01 (1 H, d, *J* = 4.0 Hz), 7.75 (1 H, d, *J* = 8.0 Hz), 7.35 (1 H, d, *J* = 4.0 Hz), 7.16 (1 H, d, *J* = 8.0 Hz), 6.05 (1 H, m), 3.52 (4 H, m), 3.47 (4 H, m), 2.50–2.60 (2 H, m), 2.09–2.25 (4 H, m), 1.55–1.75 (2H, m). HRMS (ESI) *m/z*: calculated for [M + H]⁺ 431.2303, found 431.2314.

2-Amino-9-cyclopentyl-9H-pyrido[4',3':4,5]pyrrolo[2,3-d]pyrimidin-8-yl Trifluoromethanesulfonate (40). Sodium hydride (60% in oil, 16 mg) was added to a solution of compound **38** (0.10 g, 0.371 mmol) in DMF (2 mL) and stirred at 0 °C for 30 min, then *N*-phenyl-bis-(trifluoromethanesulfonimide) (0.146 g, 0.408 mmol) in DMF (1 mL) was added dropwise at 0 °C, and the resulting mixture was stirred at 0 °C for 2 h. The reaction mixture was concentrated and dissolved in DCM. The resulting organic solution was washed with

brine, dried, and concentrated. The residue was purified by flash chromatography on silica gel, eluting with DCM/MeOH/NH₄OH (100:10:1) to give compound **40** as a yellow solid (0.102 g, 67% yield). MS (ESI) *m/z*: 402.1 [M + H]⁺.

9-Cyclopentyl-8-methyl-9H-pyrido[4',3':4,5]pyrrolo[2,3-d]pyrimidin-2-amine (41). MeMgBr (3 M, in ether, 5.5 mmol, 1.8 mL) was added dropwise to a stirred solution of **40** (1.0 g, 1.8 mmol) and ferric acetylacetonate (1.93 g, 5.5 mmol) in THF (20 mL) and NMP (1 mL) under argon. The resulting mixture was stirred at room temperature for 30 min. The reaction mixture was concentrated, and the residue was purified by flash chromatography on silica gel eluting with DCM/MeOH/NH₄OH (200:10:1) to give compound **41** as a light-yellow solid (260 mg, 54% yield). ¹H NMR (400 MHz, CDCl₃) δ ppm 8.90 (1 H, s), 8.33 (1 H, d, *J* = 8.0 Hz), 7.64 (1 H, d, *J* = 8.0 Hz), 5.38 (1 H, quin, *J* = 8.6 Hz), 5.15 (2 H, br s), 3.01 (3 H, s), 2.56–2.86 (2 H, m), 1.96–2.23 (4 H, m), 1.67–1.89 (2 H, m). MS (ESI) *m/z*: 268.1 [M + H]⁺.

9-Cyclopentyl-8-methyl-N-(5-(1-piperazinyl)-2-pyridinyl)-9H-pyrido[4',3':4,5]pyrrolo[2,3-d]pyrimidin-2-amine (4). Compound **4** was prepared according to the methods described in the synthesis of **1**. ¹H NMR (500 MHz, CD₃OD) δ ppm 9.01 (1 H, s), 8.36 (1 H, s), 8.29 (1 H, d, *J* = 8.0 Hz), 8.01 (1 H, d, *J* = 4.0 Hz), 7.62 (1 H, d, *J* = 8.0 Hz), 7.28 (1 H, d, *J* = 4.0 Hz), 5.36 (1 H, m), 3.09 (4 H, m), 3.02 (4 H, m), 2.95 (3 H, s), 2.73–2.70 (2 H, m), 2.09–1.98 (4 H, m), 1.80 (2 H, m). HRMS (ESI) *m/z*: calculated for [M + H]⁺ 429.2510, found 429.2527.

8-Cyano-9-cyclopentyl-9H-pyrido[4',3':4,5]pyrrolo[2,3-d]pyrimidin-2-amine (48). A mixture of **47** (1.50 g, 5.53 mmol) and tetraethylammonium cyanide (1.30 g, 8.29 mmol) in DMF (10 mL) was heated at 150 °C under microwave irradiation for 2 h. The reaction mixture was concentrated under reduced pressure and the residue was purified by flash chromatography on silica gel, eluting with DCM/MeOH/NH₄OH (100:10:1) to give **48** as a tan solid (1.17 g, 76% yield). ¹H NMR (400 MHz, DMSO-*d*₆) δ ppm 9.17 (1 H, s), 8.49 (1 H, d, *J* = 5.1 Hz), 8.25 (1 H, d, *J* = 5.1 Hz), 7.24 (2 H, br s), 5.59 (1 H, m), 2.49–2.56 (2 H, m), 2.05–2.14 (4 H, m), 1.70–1.75 (2 H, m). MS (ESI) *m/z*: 279.2 [M + H]⁺.

9-Cyclopentyl-2-((5-(1-piperazinyl)-2-pyridinyl)amino)-9H-pyrido[4',3':4,5]pyrrolo[2,3-d]pyrimidine-8-carbonitrile (6). Compound **6** was prepared according to the methods described in the synthesis of **1**. ¹H NMR (500 MHz, DMSO-*d*₆) δ ppm 10.42 (1 H, br s), 9.40–9.49 (1 H, m), 8.67–8.80 (2 H, m), 8.58–8.65 (1 H, m), 8.39–8.48 (1 H, m), 8.09–8.16 (1 H, m), 7.98–8.07 (1 H, m), 5.62–5.73 (1 H, m), 3.34–3.44 (5 H, m), 3.25–3.34 (4 H, m), 2.64 (2 H, m), 2.01–2.20 (4 H, m), 1.68–1.80 (2 H, m). HRMS (ESI) *m/z*: calculated for [M + H]⁺ 440.2307, found 440.2302.

N⁴-Cyclopentyl-5-(3,6-dimethoxy-4-pyridazinyl)-2,4-pyrimidine-diamine (50). A solution of *n*BuLi (2.5 M solution in hexanes) (7.5 mL, 19 mmol) was added to a cold (0 °C) solution of 2,2,6,6-tetramethylpiperidine (3.4 mL, 20 mmol) in THF (24 mL). The resulting mixture was allowed to stand at 0 °C for 30 min. The ice-water bath was then replaced with a dry ice–2-propanol bath. A precooled solution of 3,6-dimethoxy-pyridazine (2.40 g, 17 mmol) in THF (40 mL) was added through a cannula over a period of 30 min. The resulting mixture was stirred at –70 °C for 1.5 h. A solution of zinc(II) chloride (0.5 M in THF) (34 mL, 17 mmol) was added through a syringe over a period of 15 min. The cold bath was removed, and the resulting mixture was allowed to warm up to rt. A solution of compound **44a** (1.7 g, 5.7 mmol) and Pd₂(PPh₃)₄ (0.33 g, 0.29 mmol) in THF (20 mL) was added, and the resulting mixture was heated at reflux for 18 h. Upon workup, the crude mixture was cooled in an ice-water bath before being poured onto ice and saturated NH₄Cl aqueous solution and extracted with ethyl acetate (2×). The combined organics were dried over sodium sulfate and concentrated in vacuo. The residue was purified by flash chromatography on silica gel, eluting with DCM/MeOH/NH₄OH (200:10:1) to give compound **50** as an off-white solid (1.2 g, 66% yield). ¹H NMR (400 MHz, DMSO-*d*₆) δ ppm 7.53 (1 H, s), 7.01 (1 H, s), 6.18–6.38 (3 H, m), 4.35–4.51 (1 H, m, *J* = 7.3, 7.3, 7.3, 7.3, 7.0 Hz), 3.95 (3 H, s), 3.91 (3 H, s), 1.77–1.90 (2 H,

m), 1.55–1.69 (2 H, m), 1.35–1.55 (4 H, m). MS (ESI) m/z : 317.2 $[M + H]^+$.

9-Cyclopentyl-3-methoxy-9H-pyrimido[5',4':4,5]pyrrolo[2,3-c]-pyridazin-7-amine (51). To a 35 mL microwave reaction vessel was added compound **50** (200 mg, 0.63 mmol) followed by THF (15 mL) and sodium hydride (60% in mineral oil, 0.063 g, 1.6 mmol). The resulting mixture was stirred at room temperature for 10 min to allow gas release. The vessel was then subjected to microwave irradiation at 150 °C for an hour. The reaction mixture was concentrated, and the residue was purified by flash chromatography on silica gel eluting with 2% methanol in DCM to give compound **51** as a light-yellow solid (170 mg, 95% yield). $^1\text{H NMR}$ (500 MHz, DMSO- d_6) δ ppm 8.97 (1 H, s), 7.57 (1 H, s), 7.28 (2 H, s), 5.28 (1 H, quin, $J = 8.7$ Hz), 4.02 (3 H, s), 2.38–2.46 (2 H, m), 1.89–2.10 (4 H, m), 1.62–1.78 (2 H, m). MS (ESI) m/z : 285.1 $[M + H]^+$.

7-Amino-9-cyclopentyl-9H-pyrimido[5',4':4,5]pyrrolo[2,3-c]-pyridazin-3-yl Trifluoromethanesulfonate (52). A mixture of compound **51** (0.17 g, 0.60 mmol) and pyridine hydrochloride (0.69 g, 6.0 mmol) was heated at 200 °C overnight. After cooling to room temperature, the mixture was dissolved in THF (6 mL). Triethylamine (1.3 mL, 9.0 mmol), *N,N*-dimethylpyridin-4-amine (7.3 mg, 0.060 mmol), and *N*-phenyltrifluoromethanesulfonimide (0.54 g, 1.5 mmol) were added at room temperature. The resulting mixture was sonicated for 10 min and stirred for 2 h. The reaction mixture was concentrated, and the residue was purified by flash chromatography on silica gel eluting with 15–65% ethyl acetate in hexane to give compound **52** as an off-white solid (150 mg, 62% yield). MS (ESI) m/z : 403.0 $[M + H]^+$.

9-Cyclopentyl-9H-pyrimido[5',4':4,5]pyrrolo[2,3-c]pyridazin-7-amine (53). To a 25 mL single-necked round-bottom flask were added compound **52** (94 mg, 234 μmol), palladium diacetate (21 mg, 93 μmol), and 1,1'-bis(diphenylphosphino)ferrocene (130 mg, 234 μmol). The flask was subjected to three cycles of evacuation and backfilling with N_2 . DMF (3 mL) was added under N_2 , followed by triethylamine (715 μL , 5140 μmol) and formic acid (176 μL , 4.67 mmol). The resulting mixture was stirred at 65 °C for 1.5 h. The mixture was poured into ice and saturated NaHCO_3 aqueous solution, then extracted with 10% *i*-PrOH/DCM (2 \times). The combined organics were dried over sodium sulfate and concentrated in vacuo. The residue was purified by flash chromatography on silica gel eluting with DCM/MeOH/ NH_4OH (200:10:1) to give compound **53** as a reddish solid (48 mg, 80% yield). $^1\text{H NMR}$ (400 MHz, DMSO- d_6) δ ppm 9.08 (1 H, s), 9.01 (1 H, d, $J = 5.1$ Hz), 8.07 (1 H, d, $J = 5.1$ Hz), 7.28 (2 H, s), 5.42 (1 H, quin, $J = 8.6$ Hz), 2.40–2.49 (2 H, m), 1.92–2.14 (4 H, m), 1.63–1.80 (2 H, m). MS (ESI) m/z : 255.1 $[M + H]^+$.

9-Cyclopentyl-*N*-(5-(1-piperazinyl)-2-pyridinyl)-9H-pyrimido[5',4':4,5]pyrrolo[2,3-c]pyridazin-7-amine (7). Compound **7** was prepared using chemistry similar to that described in the synthesis of **1**. $^1\text{H NMR}$ (400 MHz, CD_3OD) δ ppm 9.47 (1 H, s), 9.23 (1 H, d, $J = 5.5$ Hz), 8.49 (1 H, d, $J = 5.5$ Hz), 7.99–8.11 (2 H, m), 7.75 (1 H, d, $J = 9.4$ Hz), 5.68 (1 H, quin, $J = 8.5$ Hz), 3.49–3.58 (4 H, m), 3.41–3.49 (4 H, m), 2.50–2.71 (2 H, m), 2.12–2.29 (4 H, m), 1.76–1.94 (2 H, m). HRMS (ESI) m/z : calculated for $[M + H]^+$ 416.2307, found 416.2310.

(*S*)-2-(2-((5-(Piperazin-1-yl)pyridin-2-yl)amino)-9H-pyrido[4',3':4,5]pyrrolo[2,3-d]pyrimidin-9-yl)propan-1-ol (8). Compound **8** was prepared using chemistry similar to that described in the synthesis of **1**. $^1\text{H NMR}$ (400 MHz, CD_3OD) δ ppm 9.66 (1 H, s), 9.40 (1 H, s), 8.68 (1 H, d, $J = 5.3$ Hz), 8.64 (1 H, d, $J = 5.3$ Hz), 8.05–8.11 (3 H, m), 7.77 (1 H, d, $J = 9.8$ Hz), 5.29 (1 H, m), 4.38 (1 H, dd, $J = 12.0$, 8.0 Hz), 4.03 (1 H, dd, $J = 8.0$, 4.0 Hz), 3.50–3.57 (4 H, m), 3.40–3.47 (4 H, m), 1.79 (3 H, d, $J = 8.0$ Hz). HRMS (ESI) m/z : calculated for $[M + H]^+$ 405.2147, found 405.2127.

4-[2-(5-Piperazin-1-yl-pyridin-2-ylamino)-pyrido[4',3':4,5]pyrrolo[2,3-d]pyrimidin-9-yl]-trans-cyclohexanol (9). Compound **9** was prepared using chemistry similar to that described in the synthesis of **1**. $^1\text{H NMR}$ (500 MHz, CD_3OD) δ ppm 9.62 (1 H, s), 9.42 (1 H, s), 8.64 (2 H, s), 8.11 (1 H, d, $J = 2.5$ Hz), 8.02 (1 H, d, $J = 10.0$ Hz), 7.87 (1 H, d, $J = 10.0$ Hz), 4.98 (1 H, m), 3.89 (1 H, m), 3.55 (4 H, m), 3.47 (4 H, m), 2.77 (2 H, m), 2.21 (1 H, d, $J = 15$ Hz), 2.05 (2 H,

m), 1.86 (1 H, m), 1.65 (2 H, m). HRMS (ESI) m/z : calculated for $[M + H]^+$ 445.2459, found 445.2458.

(9-Cyclohexyl-9H-pyrido[4',3':4,5]pyrrolo[2,3-d]pyrimidin-2-yl)-(5-piperazin-1-yl-pyridin-2-yl)-amine (10). Compound **10** was prepared using chemistry similar to that described in the synthesis of **1**. $^1\text{H NMR}$ (500 MHz, DMSO- d_6) δ ppm 9.56 (1 H, s), 9.47 (1 H, s), 8.77 (1 H, d, $J = 6.1$ Hz), 8.65 (1 H, d, $J = 6.1$ Hz), 8.10 (1 H, dd, $J = 9.5$, 2.7 Hz), 8.00 (1 H, d, $J = 2.7$ Hz), 7.54 (1 H, s), 7.42 (1 H, d, $J = 9.5$ Hz), 4.77–4.84 (1 H, m), 3.50–3.54 (4 H, m), 3.43–3.48 (4 H, m), 2.31–2.44 (2 H, m), 2.04–2.16 (4 H, m), 1.86–1.95 (1 H, m), 1.65–1.77 (2 H, m), 1.46–1.59 (1 H, m). HRMS (ESI) m/z : calculated for $[M + H]^+$ 429.2510, found 429.2507.

9-(4-Methylcyclohexyl)-*N*-(5-(1-piperazinyl)-2-pyridinyl)-9H-pyrido[4',3':4,5]pyrrolo[2,3-d]pyrimidin-2-amine (11). Compound **11** was prepared according to the methods described in the synthesis of **1**. $^1\text{H NMR}$ (500 MHz, CD_3OD) δ ppm 9.19 (1 H, s), 8.97 (1 H, s), 8.39 (1 H, d, $J = 6.1$ Hz), 8.27 (1 H, d, $J = 6.1$ Hz), 8.05 (1 H, m), 7.53 (1 H, m), 3.20 (4 H, m), 3.07 (4 H, m), 2.80 (1 H, m), 2.60 (1 H, m), 2.10 (1 H br s), 1.97 (3 H, m), 1.75 (3 H, m), 1.40 (1 H, m), 1.08–1.25 (3 H, m). HRMS (ESI) m/z : calculated for $[M + H]^+$ 443.2666, found 443.2666.

5-(3-Fluoropyridin-4-yl)-*N*⁴-((1*r*,4*r*)-4-methylcyclohexyl)-pyrimidine-2,4-diamine (55). To a solution of 2,2',6,6'-tetramethylpiperidine (997 mL, 5.87 mol, 3 equiv) in anhydrous THF (6 L) under N_2 atmosphere at 0 °C, was added *n*-BuLi (2.5 M in hexanes, 2350 mL, 5.87 mol, 3 equiv) via an addition funnel over 30 min. Upon completion of the addition, the reaction mixture was stirred at 0 °C for 1 h. The reaction mixture was cooled to –74 °C, and a solution of 3-fluoropyridine (561 g, 5.773 mol, 2.95 equiv) in anhydrous THF (500 mL) was added over 15 min, keeping the temperature below –63 °C. Upon completion of the addition, the reaction mixture was stirred at –74 °C for an additional 2 h. A solution of ZnBr_2 (1422 g, 6.32 mol, 3.22 equiv) in anhydrous THF (3 L) was then added dropwise over 35 min, keeping the temperature below –60 °C. Upon completion of the addition, the cold bath was removed and the reaction mixture was allowed to warm to room temperature. Then **44b** (650 g, 1.95 mol, 1.0 equiv) was added in one portion, followed by $\text{Pd}(\text{PPh}_3)_4$ (113 g, 97.8 mmol, 0.05 equiv). The reaction mixture was heated at reflux overnight and monitored using LCMS. Upon completion, the reaction mixture was cooled to room temperature, quenched with saturated aqueous NaHCO_3 (6 L), and extracted with ethyl acetate (2 \times 10 L). The organic extracts were washed with saturated NaHCO_3 (2 \times 2.5 L) and brine (2.5 L) and were then concentrated under vacuum. The residue was dissolved in 2N HCl (2.5 L) and washed with DCM (3 \times 1.25 L). The aqueous phase was adjusted to pH 10–12 by addition of aqueous 4N NaOH and extracted with DCM (3 \times 1.5 L). The organic extracts were washed with water (2 \times 1.25 L), dried, and concentrated to give compound **55** (540 g, 92% yield). $^1\text{H NMR}$ (300 MHz, DMSO- d_6) δ ppm 8.50 (1 H, d, $J = 6.6$ Hz), 8.37 (1 H, d, $J = 4.8$ Hz), 7.58 (1 H, s), 7.35 (1 H, dd, $J = 6.6$, 4.4 Hz), 6.24 (2 H, br s), 5.00 (1 H, d, $J = 8.4$ Hz), 3.96 (1 H, m), 1.74 (2 H, d, $J = 11.7$ Hz), 1.64 (2 H, d, $J = 12.3$ Hz), 1.30–1.18 (3H, m), 0.98 (1H, dd, $J = 12.9$, 2.7 Hz), 0.85 (3H, d, $J = 7.2$ Hz). MS m/z : 302.2 $[M + H]^+$.

9-((1*r*,4*r*)-4-Methylcyclohexyl)-9H-pyrido[4',3':4,5]pyrrolo[2,3-d]pyrimidin-2-amine (33d). To a solution of **55** (854 g, 2.84 mol, 1.0 equiv) in anhydrous 1-methyl-2-pyrrolidinone (8 L) under N_2 atmosphere at room temperature was added LiHMDS (1.0 M in toluene, 8.5 L, 8.5 mol, 3.0 equiv) over 30 min. Upon completion of the addition, the reaction mixture was heated at 90 °C overnight and monitored using LCMS. Upon completion, the reaction mixture was cooled to room temperature, quenched with ice-cold water (10 L), and extracted with ethyl acetate (12 L). The organic phase was washed with saturated aqueous NaHCO_3 (2 \times 4 L) and water (3 \times 2 L). The aqueous layers were combined and back-extracted with ethyl acetate (2 \times 15 L). The organic layers were combined, dried over Na_2SO_4 , and concentrated under reduced pressure. The solid thus obtained was suspended in DCM (2.5 L) and agitated using a rotary evaporator for 30 minutes. The solid was collected by filtration, washed with DCM, and dried to afford compound **33d** (400 g). The mother liquor was purified by column chromatography (eluting with DCM/MeOH =

50:1) to afford, after triturating with DCM (750 mL), additional compound **33d** (277 g, total: 677 g, 84% yield). ¹H NMR (400 MHz, DMSO-*d*₆) δ ppm 8.95 (1 H, s), 8.92 (1 H, s), 8.46 (1 H, d, *J* = 5.3 Hz), 7.78 (1 H, d, *J* = 5.3 Hz), 5.22 (2 H, br s), 4.72–4.88 (1 H, m), 2.45 (2 H, qd, *J* = 12.9, 4.0 Hz), 1.82–2.12 (4 H, m), 1.56–1.71 (1 H, m), 1.21–1.42 (2 H, m), 1.02 (3 H, d, *J* = 6.5 Hz). HRMS (ESI) *m/z*: calculated for [M + H]⁺ 282.1713, found 282.1709.

9-((1*r*,4*r*)-4-Methylcyclohexyl)-N-(5-(piperazin-1-yl)pyridin-2-yl)-9H-pyrido[4',3':4,5]pyrrolo[2,3-*d*]pyrimidin-2-amine (**12**). Compound **12** was prepared according to the methods described in the synthesis of **1**. ¹H NMR (500 MHz, DMSO-*d*₆) δ ppm 9.76 (1 H, s), 9.26 (1 H, s), 9.10 (1 H, s), 8.42 (1 H, d, *J* = 5.1 Hz), 8.20 (1 H, d, *J* = 9.0 Hz), 7.98–8.07 (2 H, m), 7.44 (1 H, dd, *J* = 9.0, 5.1 Hz), 4.80 (1 H, m), 3.04–3.06 (4 H, m), 2.06–2.08 (4 H, m), 2.55–2.61 (2 H, m), 1.80–1.93 (4 H, m), 1.66 (1 H, m), 1.21–1.29 (2 H, m), 1.01 (3 H, d, *J* = 6.4 Hz). HRMS (ESI) *m/z*: calculated for [M + H]⁺ 443.2666, found 443.2681.

9-(4,4-Dimethylcyclohexyl)-N-(5-(1-piperazinyl)-2-pyridinyl)-9H-pyrido[4',3':4,5]pyrrolo[2,3-*d*]pyrimidin-2-amine (**13**). Compound **13** was prepared according to the methods described in the synthesis of **1**. ¹H NMR (400 MHz, DMSO-*d*₆) δ ppm 10.35 (1 H, s), 9.52 (1 H, s), 9.35 (1 H, s), 8.62 (1 H, d, *J* = 5.9 Hz), 8.49 (1 H, d, *J* = 5.9 Hz), 8.15 (1 H, d, *J* = 2.9 Hz), 8.04 (1 H, d, *J* = 9.0 Hz), 7.51 (1 H, dd, *J* = 9.0, 2.9 Hz), 4.66–4.79 (1 H, m), 3.34–3.43 (4 H, m), 3.30 (4 H, br s), 2.62–2.77 (2 H, m), 1.73 (2 H, d, *J* = 11.3 Hz), 1.46–1.63 (4 H, m), 1.11 (3 H, s), 1.02 (3 H, s). HRMS (ESI) *m/z*: calculated for [M + H]⁺ 457.2822, found 457.2806.

9-(3,3-Dimethylcyclohexyl)-N-(5-(piperazin-1-yl)pyridin-2-yl)-9H-pyrido[4',3':4,5]pyrrolo[2,3-*d*]pyrimidin-2-amine (**14**). Compound **14** was prepared according to the methods described in the synthesis of **1**. ¹H NMR (400 MHz, CD₃OD) δ ppm 9.70 (1 H, s), 9.51 (1 H, s), 8.75 (1 H, d, *J* = 5.3 Hz), 8.68 (1 H, d, *J* = 5.3 Hz), 8.17 (1 H, dd, *J* = 9.8, 3.2 Hz), 8.06 (1 H, d, *J* = 3.2 Hz), 7.74 (1 H, d, *J* = 9.8 Hz), 5.21 (1 H, m), 3.52–3.57 (4 H, m), 3.44–3.47 (4 H, m), 2.45–2.55 (2 H, m), 2.03 (1 H, m), 1.82–1.91 (2 H, m), 1.71 (1 H, m), 1.47–1.57 (2 H, m), 1.21 (3 H, s), 1.10 (3 H, s). HRMS (ESI) *m/z*: calculated for [M + H]⁺ 457.2822, found 457.2829.

9-((1*r*,4*r*)-4-Methylcyclohexyl)-N-(6-(piperazin-1-yl)pyridin-3-yl)-9H-pyrido[4',3':4,5]pyrrolo[2,3-*d*]pyrimidin-2-amine (**15**). Compound **15** was prepared according to the methods described in the synthesis of **1**. ¹H NMR (400 MHz, DMSO-*d*₆) δ ppm 9.61 (1 H, s), 9.19 (1 H, s), 9.05 (1 H, s), 8.53 (1 H, s), 8.39 (1 H, d, *J* = 5.1 Hz), 7.87–8.01 (2 H, m), 6.81 (1 H, d, *J* = 9.0 Hz), 4.75 (1 H, m), 3.28–3.41 (4 H, m), 2.73–2.88 (4 H, m), 2.53–2.62 (2 H, m), 1.80–1.87 (4 H, m), 1.67 (1 H, m), 1.15–1.25 (2 H, m), 0.99 (3 H, d, *J* = 6.5 Hz). HRMS (ESI) *m/z*: calculated for [M + H]⁺ 443.2666, found 443.2680.

9-((1*r*,4*r*)-4-Methylcyclohexyl)-N-(6-(piperazin-1-yl)pyridazin-3-yl)-9H-pyrido[4',3':4,5]pyrrolo[2,3-*d*]pyrimidin-2-amine (**16**). Compound **16** was prepared from **33d** and **58e** using chemistry similar to that described in the synthesis of **1**. ¹H NMR (500 MHz, DMSO-*d*₆) δ ppm 10.86 (1 H, br s), 9.51 (1 H, s), 9.40 (1 H, s), 8.98 (1 H, br s), 8.62 (1 H, d, *J* = 5.9 Hz), 8.47 (1 H, d, *J* = 5.9 Hz), 8.25 (1 H, d, *J* = 9.8 Hz), 7.58 (1 H, d, *J* = 9.8 Hz), 4.82 (1 H, t, *J* = 3.8 Hz), 3.75–3.84 (4 H, m), 3.27–3.33 (4 H, m), 2.49–2.55 (2 H, m), 1.87 (4 H, ddd, *J* = 10.1, 1.4, 1.2 Hz), 1.61 (1 H, m), 1.17–1.25 (2 H, m), 0.99 (3 H, d, *J* = 6.4 Hz). HRMS (ESI) *m/z*: calculated for [M + H]⁺ 444.2619, found 444.2617.

8-(6-Chloropyridin-3-yl)-1,4-dioxo-8-azaspiro[4.5]decane (**59a**). To a solution of 5-bromo-2-chloropyridine (7.70 g, 40 mmol) in toluene (200 mL) were added 1,4-dioxo-8-azaspiro[4.5]decane (6.30 g, 44 mmol), sodium *t*-butoxide (5.76 g, 60 mmol), Pd₂dba₃ (548 mg, 0.60 mmol), and XantPhos (1388 mg, 2.40 mmol). The mixture was purged with argon then heated at 100 °C for 5 h. The reaction mixture was then cooled to room temperature, diluted with ethyl acetate, and washed with water. The organic layer was concentrated, and the residue was purified by flash chromatography on silica gel, eluting with 15–50% ethyl acetate in hexanes to give **59a** as a light-yellow solid (7.77 g, 76% yield). ¹H NMR (400 MHz, CDCl₃) δ ppm 8.03 (1 H, d, *J* = 2.2 Hz), 7.19 (1 H, dd, *J* = 8.0, 2.2 Hz), 7.15 (1 H, d, *J* = 8.0 Hz),

4.0 (4 H, s), 3.32–3.34 (4 H, m), 1.82–1.85 (4 H, m). MS (ESI) *m/z*: 255.2 [M + H]⁺.

1-(6-((9-((1*r*,4*r*)-4-Methylcyclohexyl)-9H-pyrido[4',3':4,5]pyrrolo[2,3-*d*]pyrimidin-2-yl)amino)pyridin-3-yl)piperidin-4-one (**60a**). To a solution of **33d** (563 mg, 2.0 mmol) in 1,4-dioxane (20 mL) were added **59a** (611 mg, 2.40 mmol), Pd₂dba₃ (92 mg, 0.10 mmol), XantPhos (175 mg, 0.30 mmol), and sodium *t*-butoxide (290 mg, 3.0 mmol). The reaction mixture was purged with argon, then heated at 150 °C under microwave irradiation for 2 h. The reaction mixture was subjected to flash chromatography on silica gel to give *N*-(5-(1,4-dioxo-8-azaspiro[4.5]decane-8-yl)pyridin-2-yl)-9-((1*r*,4*r*)-4-methylcyclohexyl)-9H-pyrido[4',3':4,5]pyrrolo[2,3-*d*]pyrimidin-2-amine as a yellow solid (1 g, 90% purity). ¹H NMR (500 MHz, CDCl₃) δ ppm 9.07 (1 H, s), 8.96 (1 H, s), 8.49 (1 H, d, *J* = 5.1 Hz), 8.42 (1 H, d, *J* = 9.0 Hz), 8.14 (1 H, br s), 8.09 (1 H, d, *J* = 3.2 Hz), 7.32 (1 H, d, *J* = 5.1 Hz), 7.40 (1 H, dd, *J* = 9.0, 3.2 Hz), 4.75 (1 H, m), 4.02 (4 H, s), 3.31–3.33 (4 H, m), 2.51–2.68 (2 H, m), 1.97–2.01 (4 H, m), 1.90–1.92 (4 H, m), 1.87 (1 H, m), 1.18–1.41 (2 H, m), 1.07 (3 H, d, *J* = 6.6 Hz). MS (ESI) *m/z*: 500.2 [M + H]⁺. The yellow solid was dissolved in THF (10 mL) and 3 N HCl (10 mL), then stirred at 60 °C overnight. To the reaction mixture was added 1 N NaOH (30 mL), and the resulting mixture was extracted with DCM. The organic layer was dried over MgSO₄ and concentrated under reduced pressure to give crude **60a** as a yellow solid (1.1 g, 80% purity) that was used in the next step without further purification. MS (ESI) *m/z*: 456.2 [M + H]⁺.

N-(5-(4-Aminopiperidin-1-yl)pyridin-2-yl)-9-((1*r*,4*r*)-4-methylcyclohexyl)-9H-pyrido[4',3':4,5]pyrrolo[2,3-*d*]pyrimidin-2-amine (**17**). To a solution of **60a** (285 mg, 80% purity, 0.5 mmol) in methanol (10 mL) were added molecular sieves (3 Å) (1.5 g) and ammonium acetate (385 mg, 5 mmol), and the mixture thus obtained was stirred at room temperature for 20 min. To the reaction mixture was added sodium cyanoborohydride (126 mg, 4 mmol), and the mixture was stirred at 60 °C for 2 h. The reaction mixture was filtered, and the filtrate was concentrated under reduced pressure. The residue was purified by flash chromatography on silica gel, eluting with DCM/MeOH/NH₄OH to give **17** as a light-yellow solid (78 mg, 34% yield). ¹H NMR (500 MHz, DMSO-*d*₆) δ ppm 9.73 (1 H, s), 9.25 (1 H, s), 9.10 (1 H, s), 8.42 (1 H, d, *J* = 5.1 Hz), 8.17 (1 H, d, *J* = 9.0 Hz), 8.01–8.04 (2 H, m), 7.42 (1 H, dd, *J* = 9.0, 3.2 Hz), 4.79 (1 H, m), 3.60 (2 H, ddd, *J* = 12.8, 4.0, 3.9 Hz), 3.20–3.44 (2 H, m), 2.65–2.89 (3 H, m), 2.51–2.65 (2 H, m), 1.80–1.89 (6 H, m), 1.68 (1 H, m), 1.31–1.44 (2 H, m), 1.12–1.31 (2 H, m), 1.00 (3 H, d, *J* = 6.6 Hz). HRMS (ESI) *m/z*: calculated for [M + H]⁺ 457.2822, found 457.2811.

1-(6-Chloropyridin-3-yl)-*N,N*-dimethylpiperidin-4-amine (**58a**). Compound **58a** was prepared according to the methods described in the synthesis of **59a** with a 93% yield. ¹H NMR (500 MHz, CDCl₃) δ ppm 8.02 (1 H, d, *J* = 2.9 Hz), 7.19 (1 H, dd, *J* = 9.8, 2.9 Hz), 7.15 (1 H, d, *J* = 9.8 Hz), 3.64–3.74 (2 H, m), 2.75–2.81 (2 H, m), 2.31 (6 H, s), 2.16–2.30 (1 H, m), 1.91–1.95 (2 H, m), 1.55–1.78 (2 H, m). MS (ESI) *m/z*: 240.1 [M + H]⁺.

N-(5-(4-(Dimethylamino)piperidin-1-yl)pyridin-2-yl)-9-((1*r*,4*r*)-4-methylcyclohexyl)-9H-pyrido[4',3':4,5]pyrrolo[2,3-*d*]pyrimidin-2-amine (**18**). To a solution of **33d** (110 mg, 0.39 mmol) in 1,4-dioxane (4 mL) were added **58a** (112 mg, 0.47 mmol), Pd₂dba₃ (18 mg), XantPhos (35 mg), and sodium *t*-butoxide (43 mg, 0.59 mmol). The reaction mixture was purged with argon then heated at 150 °C under microwave irradiation for 1 h. The reaction mixture was purified by flash chromatography on silica gel, eluting with DCM/MeOH/NH₄OH (100:10:1) to give **18** as a yellow solid (140 mg, 74% yield). ¹H NMR (400 MHz, DMSO-*d*₆) δ ppm 9.81 (1 H, s), 9.28 (1 H, s), 9.13 (1 H, s), 8.44 (1 H, d, *J* = 5.3 Hz), 8.21 (1 H, d, *J* = 9.2 Hz), 8.08 (1 H, d, *J* = 3.1 Hz), 8.06 (1 H, d, *J* = 5.3 Hz), 7.51 (1 H, dd, *J* = 9.2, 3.1 Hz), 4.78 (1 H, m), 3.82–3.85 (2 H, m), 2.77 (6 H, s), 2.72–2.77 (3 H, m), 2.51–2.65 (2 H, m), 2.10–2.14 (2 H, m), 1.72–1.91 (6 H, m), 1.64 (1 H, m), 1.20–1.29 (2 H, m), 1.01 (3 H, d, *J* = 6.5 Hz). HRMS (ESI) *m/z*: calculated for [M + H]⁺ 485.3134, found 485.3128.

N-(6-(4-(Dimethylamino)piperidin-1-yl)pyridazin-3-yl)-9-((1*r*,4*r*)-4-methylcyclohexyl)-9H-pyrido[4',3':4,5]pyrrolo[2,3-*d*]pyrimidin-2-amine (**19**). Compound **19** was prepared according to the methods described in the synthesis of **18**. ¹H NMR (500 MHz, CDCl₃) δ ppm

9.07 (1 H, s), 8.98 (1 H, s), 8.55 (1 H, d, $J = 9.8$ Hz), 8.51 (1 H, d, $J = 5.4$ Hz), 8.25 (1 H, s), 7.84 (1 H, d, $J = 5.4$ Hz), 7.10 (1 H, d, $J = 9.8$ Hz), 4.77 (1 H, m), 4.34–4.38 (2 H, m), 2.92–3.04 (2 H, m), 2.46–2.62 (2 H, m), 2.41 (1 H, m), 2.33 (6 H, s), 1.82–2.03 (6 H, m), 1.55–1.69 (3 H, m), 1.24–1.38 (2 H, m), 1.07 (3 H, d, $J = 6.4$ Hz). HRMS (ESI) m/z : calculated for $[M + H]^+$ 486.3087, found 486.3094.

N-(5-(4-(Dimethylamino)piperidin-1-yl)-6-fluoropyridin-2-yl)-9-((1*r*,4*r*)-4-methylcyclohexyl)-9*H*-pyrido[4',3':4,5]pyrrolo[2,3-*d*]pyrimidin-2-amine (**20**). Compound **20** was prepared according to the methods described in the synthesis of **18**. ^1H NMR (400 MHz, CD_3OD) δ ppm 9.44 (1 H, s), 9.27 (1 H, s), 8.39–8.58 (2 H, m), 8.26 (1 H, d, $J = 8.4$ Hz), 7.63 (1 H, m), 4.98 (1 H, m), 3.59–3.66 (2 H, m), 3.39 (1 H, m), 2.96 (6 H, s), 2.85–3.00 (2 H, m), 2.62–2.80 (2 H, m), 2.20–2.27 (2 H, m), 1.90–2.10 (6 H, m), 1.73 (1 H, m), 1.28–1.47 (2 H, m), 1.10 (3 H, d, $J = 5.6$ Hz). HRMS (ESI) m/z : calculated for $[M + H]^+$ 503.3040, found 503.3044.

N-(5-(4-(Dimethylamino)piperidin-1-yl)-6-methoxy-pyridin-2-yl)-9-((1*r*,4*r*)-4-methylcyclohexyl)-9*H*-pyrido[4',3':4,5]pyrrolo[2,3-*d*]pyrimidin-2-amine (**21**). Compound **21** was prepared according to the methods described in the synthesis of **18**. ^1H NMR (500 MHz, CDCl_3) δ ppm 9.06 (1 H, s), 8.97 (1 H, s), 8.49 (1 H, d, $J = 5.1$ Hz), 7.98 (1 H, d, $J = 8.3$ Hz), 7.90 (1 H, s), 7.82 (1 H, d, $J = 5.1$ Hz), 7.26 (1 H, d, $J = 8.3$ Hz), 4.78 (1 H, m), 3.99 (3 H, s), 3.40–3.62 (2 H, m), 2.58–2.77 (4 H, m), 2.35 (6 H, s), 2.34 (1 H, m), 1.91–2.10 (6 H, m), 1.76–1.82 (2 H, m), 1.66 (1 H, m), 1.18–1.39 (2 H, m), 1.07 (3 H, d, $J = 6.6$ Hz). HRMS (ESI) m/z : calculated for $[M + H]^+$ 515.3239, found 515.3239.

(*R*)-1-(Methyl(1-(6-((9-((1*r*,4*r*)-4-methylcyclohexyl)-9*H*-pyrido[4',3':4,5]pyrrolo[2,3-*d*]pyrimidin-2-yl)amino)pyridazin-3-yl)-piperidin-4-yl)amino)propan-2-ol (**22**). Compound **22** was prepared according to the methods described in the synthesis of **17**. ^1H NMR (500 MHz, CDCl_3) δ ppm 9.09 (1 H, s), 8.98 (1 H, s), 8.56 (1 H, d, $J = 9.8$ Hz), 8.51 (1 H, d, $J = 5.1$ Hz), 8.41 (1 H, s), 7.84 (1 H, d, $J = 5.1$ Hz), 7.10 (1 H, d, $J = 9.8$ Hz), 5.30 (1 H, s), 4.77 (1 H, m), 4.32–4.56 (2 H, m), 3.78 (1 H, ddd, $J = 10.4, 6.1, 3.1$ Hz), 2.80–3.03 (2 H, m), 2.69 (1 H, m), 2.46–2.62 (2 H, m), 2.41 (1 H, m), 2.31 (3 H, s), 2.30 (1 H, m), 1.95–2.00 (4 H, m), 1.81 (1 H, m), 1.56–1.77 (3 H, m), 1.20–1.38 (2 H, m), 1.14 (3 H, d, $J = 6.1$ Hz), 1.06 (3 H, d, $J = 6.4$ Hz). HRMS (ESI) m/z : calculated for $[M + H]^+$ 530.3348, found 530.3349.

2-Hydroxy-1-(4-(6-((9-((1*r*,4*r*)-4-methylcyclohexyl)-9*H*-pyrido[4',3':4,5]pyrrolo[2,3-*d*]pyrimidin-2-yl)amino)pyridazin-3-yl)-piperazin-1-yl)ethanone (**23**). To a solution of **16** (108 mg, 0.243 mmol) in DMF (10 mL) were added glycolic acid (0.023 mL, 0.365 mmol), PyBroP (170 mg, 0.365 mmol), and DIPEA (0.127 mL, 0.730 mmol), and the resulting mixture was stirred at room temperature overnight. The reaction mixture was concentrated under reduced pressure, and the residue was purified by flash chromatography on silica gel, eluting with DCM/MeOH/ NH_4OH (100:10:1) to give compound **23** as a yellow solid (85 mg, 70% yield). ^1H NMR (400 MHz, $\text{DMSO}-d_6$) δ ppm 10.25 (1 H, s), 9.27 (1 H, s), 9.11 (1 H, s), 8.43 (1 H, d, $J = 5.1$ Hz), 8.27 (1 H, d, $J = 9.8$ Hz), 8.04 (1 H, d, $J = 5.1$ Hz), 7.46 (1 H, d, $J = 9.8$ Hz), 4.80 (1 H, m), 4.64 (1 H, t, $J = 8.2$ Hz), 4.16 (2 H, d, $J = 8.2$ Hz), 3.50–3.65 (8 H, m), 2.50–2.55 (2 H, m), 1.80–1.90 (4 H, m), 1.66 (1 H, m), 1.20–1.27 (2 H, m), 0.99 (3 H, d, $J = 6.5$ Hz). HRMS (ESI) m/z : calculated for $[M + H]^+$ 502.2673, found 502.2676.

(1-(6-Chloropyridazin-3-yl)piperidin-4-yl)methanol (**62**). A mixture of 3,6-dichloropyridazine (13.58 g, 91 mmol), DIPEA (11.78 g, 15.92 mL, 91 mmol), and 4-piperidinmethanol (10.50 g, 91 mmol) was heated at 90 °C for 2 h. The mixture was purified by flash chromatography on silica gel, eluting with 40–100% ethyl acetate in hexanes to give **62** as a white solid (20.28 g, 98% yield). ^1H NMR (400 MHz, CDCl_3) δ ppm 7.19 (1 H, d, $J = 9.6$ Hz), 6.93 (1 H, d, $J = 9.6$ Hz), 4.27–4.45 (2 H, m), 3.56 (2 H, d, $J = 6.1$ Hz), 2.84–3.12 (2 H, m), 1.65–1.98 (4 H, m), 1.10–1.45 (2 H, m). MS (ESI) m/z : 228.1 $[M + H]^+$.

3-Chloro-6-(4-((methylthio)methyl)piperidin-1-yl)pyridazine (**63**). To a solution of **62** (1.55 g, 6.81 mmol) in DCM (10 mL) were added triethylamine (1.14 mL, 8.17 mmol) and methane sulfonyl chloride (0.579 mL, 7.49 mmol). The mixture was stirred for 3 h at room

temperature then purified by flash chromatography on silica gel to give (1-(6-chloropyridazin-3-yl)piperidin-4-yl)methyl methanesulfonate (2.05 g, 98% yield, MS (ESI) m/z : 306.0 $[M + H]^+$). The mesylate (500 mg, 1.64 mmol) was dissolved in DMF (2 mL), and sodium methanethiolate (115 mg, 1.64 mmol) was added. The mixture thus obtained was stirred overnight at room temperature. The reaction mixture was diluted with ethyl acetate and washed with water and brine, then dried over MgSO_4 . The solvent was evaporated under reduced pressure to give crude **63** (500 mg, 85% purity) which was used in next step without further purification. MS (ESI) m/z : 258.0 $[M + H]^+$.

3-Chloro-6-(4-((methylsulfonyl)methyl)piperidin-1-yl)pyridazine (**64**). To a solution of **63** (500 mg, 85% purity, 1.64 mmol) in 90% methanol in water was added oxone (2.22 g, 3.61 mmol). The reaction mixture was stirred overnight at room temperature, then diluted with ethyl acetate, washed with water and brine, and then dried. The solvent was evaporated and the residue was purified by flash chromatography on silica gel eluting with DCM/MeOH/ NH_4OH (200:10:1) to give compound **64** (436 mg, 92% yield). MS (ESI) m/z : 290.0 $[M + H]^+$.

9-((1*r*,4*r*)-4-Methylcyclohexyl)-*N*-(6-(4-((methylsulfonyl)methyl)piperidin-1-yl)pyridazin-3-yl)-9*H*-pyrido[4',3':4,5]pyrrolo[2,3-*d*]pyrimidin-2-amine (**24**). Compound **24** was prepared from **33d** and **64** using similar chemistry described in the synthesis of **1**. ^1H NMR (500 MHz, CDCl_3) δ ppm 9.07 (1 H, s), 8.99 (1 H, s), 8.58 (1 H, d, $J = 10.0$ Hz), 8.51 (1 H, d, $J = 5.3$ Hz), 7.85 (1 H, d, $J = 5.3$ Hz), 7.10 (1 H, d, $J = 10.0$ Hz), 4.78 (1 H, m), 4.29–4.37 (2 H, m), 3.00–3.09 (5 H, m), 2.98 (3 H, s), 2.40–2.60 (3 H, m), 2.09–2.16 (2 H, m), 1.94–2.06 (4 H, m), 1.58–1.65 (2 H, m), 1.24–1.36 (2 H, m), 1.07 (3 H, d, $J = 6.5$ Hz). HRMS (ESI) m/z : calculated for $[M + H]^+$ 535.2597, found 535.2601.

8-(6-Chloropyridazin-3-yl)-2-thia-8-azaspiro[4.5]decane 2,2-Dioxide (**66**). To a solution of 3,6-dichloropyridazine (5.57 g, 37.4 mmol) and 2-thia-8-azaspiro[4.5]decane 2,2-dioxide hydrochloride (**65**) (2.11 g, 9.35 mmol) in 1,4-dioxane (5 mL) was added DIPEA (5.41 mL, 32.7 mmol). The reaction mixture was heated at 80 °C overnight and then concentrated. The residue was purified by flash chromatography on silica gel, eluting with 60–100% ethyl acetate in hexanes to give **66** as a white solid (2.58 g, 91% yield). NMR (400 MHz, CDCl_3) δ ppm 7.24 (1 H, d, $J = 9.6$ Hz), 6.94 (1 H, d, $J = 9.6$ Hz), 3.95–4.04 (2 H, m), 3.35 (2 H, ddd, $J = 13.7, 10.0, 3.2$ Hz), 3.23 (2 H, s), 2.18 (2 H, t, $J = 7.6$ Hz), 1.88–1.96 (2 H, m), 1.74–1.83 (2 H, m). MS (ESI) m/z : 302.0 $[M + H]^+$.

8-(6-((9-((1*r*,4*r*)-4-Methylcyclohexyl)-9*H*-pyrido[4',3':4,5]pyrrolo[2,3-*d*]pyrimidin-2-yl)amino)pyridazin-3-yl)-2-thia-8-azaspiro[4.5]decane 2,2-Dioxide (**25**). Compound **25** was prepared from **33d** and **66** using similar chemistry described in the synthesis of **1**. ^1H NMR (500 MHz, $\text{DMSO}-d_6$) δ ppm 10.18 (1 H, s), 9.26 (1 H, s), 9.10 (1 H, s), 8.42 (1 H, d, $J = 5.3$ Hz), 8.19 (1 H, d, $J = 9.6$ Hz), 8.40 (1 H, d, $J = 5.3$ Hz), 7.44 (1 H, d, $J = 9.6$ Hz), 4.77 (1 H, m), 3.81–3.90 (2 H, m), 3.26–3.37 (2 H, m), 3.24 (2 H, t, $J = 7.6$ Hz), 3.17 (2 H, s), 2.50–2.55 (2 H, m), 2.09 (2 H, t, $J = 7.6$ Hz), 1.79–1.88 (6 H, m), 1.63–1.69 (3 H, m), 1.19–1.26 (2 H, m), 0.99 (3 H, d, $J = 6.6$ Hz). HRMS (ESI) m/z : calculated for $[M + H]^+$ 547.2597, found 547.2607.

1,8-Diazaspiro[4.5]decan-2-one hydrochloride (**68**). To a solution of **67** (268 mg, 1.06 mmol) in 1,4-dioxane (6 mL) was added 4 M HCl in dioxane (6 mL), and the solution thus obtained was stirred 2 h at 50 °C. The reaction mixture was concentrated, and the residue was dried under high vacuum to give **68** as a white solid (201 mg, 100% yield). ^1H NMR (500 MHz, $\text{DMSO}-d_6$) δ ppm 8.85 (1 H, br s), 3.05–3.15 (4 H, m), 2.22 (2 H, t, $J = 8.1$ Hz), 1.88 (2 H, t, $J = 8.1$ Hz), 1.69–1.82 (4 H, m). MS (ESI) m/z : 155.1 $[M + H]^+$.

8-(6-Chloropyridin-3-yl)-1,8-diazaspiro[4.5]decan-2-one (**69a**). Compound **69a** was prepared from **56a** and **68** using similar chemistry described in the synthesis of **34a**. ^1H NMR (500 MHz, CDCl_3) δ ppm 8.04 (1 H, d, $J = 2.7$ Hz), 2.7 (1 H, s), 7.16–7.23 (2 H, m), 6.23 (1 H, br s), 3.19–3.31 (4 H, m), 2.45 (2 H, t, $J = 8.1$ Hz), 2.04 (2 H, t, $J = 8.1$ Hz), 1.83–1.89 (4 H, m). MS (ESI) m/z : 266.0 $[M + H]^+$.

8-(6-Chloro-2-methoxy-pyridin-3-yl)-1,8-diazaspiro[4.5]decan-2-one (**69b**). Compound **69b** was prepared from **56d** and **68** using

similar chemistry described in the synthesis of **34a**. ^1H NMR (500 MHz, DMSO- d_6) δ ppm 7.95 (1 H, br s), 7.23 (1 H, d, $J = 8.1$ Hz), 6.98 (1 H, d, $J = 8.1$ Hz), 3.87 (3 H, s), 3.08–3.15 (2 H, m), 2.80–2.90 (2 H, m), 2.21 (2 H, t, $J = 8.0$ Hz), 1.86 (2 H, t, $J = 8.0$ Hz), 1.60–1.75 (4 H, m). MS (ESI) m/z : 296.1 $[\text{M} + \text{H}]^+$.

8-(6-((9-((1*r*,4*r*)-4-Methylcyclohexyl)-9*H*-pyrido[4',3':4,5]pyrrolo[2,3-*d*]pyrimidin-2-yl)amino)pyridin-3-yl)-1,8-diazaspiro[4.5]decan-2-one (26). Compound **26** was prepared from **33d** and **69a** using similar chemistry described in the synthesis of **1**. ^1H NMR (500 MHz, DMSO- d_6) δ ppm 9.73 (1 H, s), 9.26 (1 H, s), 9.10 (1 H, s), 8.42 (1 H, d, $J = 8.1$ Hz), 8.19 (1 H, d, $J = 9.8$ Hz), 8.04 (1 H, d, $J = 5.0$ Hz), 8.03 (1 H, d, $J = 8.1$ Hz), 8.00 (1 H, s), 7.48 (1 H, dd, $J = 9.8, 5.0$ Hz), 4.80 (1 H, m), 3.30–3.40 (2 H, m), 3.10–3.14 (2 H, m), 2.54–2.64 (2 H, m), 2.23 (2 H, t, $J = 8.1$ Hz), 1.90 (2 H, t, $J = 8.1$ Hz), 1.82–1.91 (4 H, m), 1.62–1.77 (5 H, m), 1.22–1.29 (2 H, m), 1.01 (3 H, d, $J = 6.5$ Hz). HRMS (ESI) m/z : calculated for $[\text{M} + \text{H}]^+$ 511.2927, found 511.2931.

8-(2-Methoxy-6-((9-((1*r*,4*r*)-4-methylcyclohexyl)-9*H*-pyrido[4',3':4,5]pyrrolo[2,3-*d*]pyrimidin-2-yl)amino)pyridin-3-yl)-1,8-diazaspiro[4.5]decan-2-one (27). Compound **27** was prepared from **33d** and **69b** using similar chemistry described in the synthesis of **1**. ^1H NMR (500 MHz, DMSO- d_6) δ ppm 9.55 (1 H, s), 9.29 (1 H, s), 9.12 (1 H, s), 8.43 (1 H, d, $J = 5.3$ Hz), 8.05 (1 H, d, $J = 5.3$ Hz), 7.97 (1 H, br s), 7.84 (1 H, d, $J = 9.8$ Hz), 7.28 (1 H, d, $J = 9.8$ Hz), 4.83 (1 H, m), 3.92 (3 H, s), 3.30–3.38 (2 H, m), 3.10–3.14 (2 H, m), 2.56–2.64 (2 H, m), 2.23 (2 H, d, $J = 8.1$ Hz), 1.90 (2 H, t, $J = 8.1$ Hz), 1.82–1.90 (4 H, m), 1.66–1.80 (5 H, m), 1.23–1.30 (2 H, m), 1.02 (3 H, d, $J = 6.5$ Hz). HRMS (ESI) m/z : calculated for $[\text{M} + \text{H}]^+$ 541.3039, found 541.3040.

***t*-Butyl 2-Chloro-7,8-dihydro-1,6-naphthyridine-6(5*H*)-carboxylate (71)**. To a slurry of 2-chloro-5,6,7,8-tetrahydro-1,6-naphthyridine hydrochloride (106.1 g, 517 mmol) and *N,N*-diisopropylethylamine (80 g, 108 mL, 621 mmol, 1.2 equiv) in DCM (1 L) was added a solution of di-*tert*-butyl dicarbonate (119 g, 543 mmol, 1.05 equiv) in DCM (100 mL) via an addition funnel within 1 h. The reaction mixture became a clear solution, and the solution thus obtained was stirred at room temperature for an additional hour and monitored using LCMS. Upon completion, the reaction mixture was concentrated. The residue was dissolved in ethyl acetate (1 L) and washed with water (3 \times 300 mL), brine (300 mL), and dried over MgSO_4 . The solvent was evaporated under vacuum to give compound **71** as an off-white solid (139 g, 100% yield). ^1H NMR (400 MHz, CDCl_3) δ ppm 7.38 (1 H, d, $J = 8.0$ Hz), 7.17 (1 H, d, $J = 8.0$ Hz), 4.57 (2 H, s), 3.73 (2 H, t, $J = 5.9$ Hz), 2.97 (2 H, t, $J = 5.9$ Hz), 1.49 (9H, s). LCMS (ESI) m/z : 269 $[\text{M} + \text{H}]^+$.

***t*-Butyl 2-((9-((1*r*,4*r*)-4-Methylcyclohexyl)-9*H*-pyrido[4',3':4,5]pyrrolo[2,3-*d*]pyrimidin-2-yl)amino)-7,8-dihydro-1,6-naphthyridine-6(5*H*)-carboxylate (72)**. To a solution of **33d** (2.81 g, 10 mmol) in 1,4-dioxane (45 mL) were added **71** (2.57 g, 9.55 mmol), XantPhos (231 mg, 0.40 mmol), and sodium *t*-butoxide (1.44 g, 15 mmol). Argon was bubbled through the mixture for 10 min. Pd2dba3 (183 mg, 0.20 mmol) was added, and argon was again bubbled through the mixture for 5 min. The reaction mixture thus obtained was stirred at 100 $^\circ\text{C}$ for 3 h, whereupon HPLC-MS analysis indicated that the reaction was complete. The reaction mixture was cooled to 40 $^\circ\text{C}$, diluted with DCM (90 mL), and treated with Si-triamine (functionalized silica gel) (2.8 g) overnight at room temperature. Celite brand filter aid 545 (6 g) was added, the mixture was filtered with a sintered glass funnel, and the solid phase was rinsed with DCM (100 mL). The filtrate was concentrated to 25 mL on a rotary evaporator and diluted with a mixture of ethyl acetate and hexane (20 mL, 4:1). The resulting slurry was stirred at room temperature for 5 h. The solid was collected by filtration, washed with a mixture of ethyl acetate and hexane (20 mL, 1:1), and air-dried for a few hours to provide compound **72** as an off-white solid (4.90 g, 100% yield). ^1H NMR (500 MHz, CD_2Cl_2) δ ppm 9.10 (1 H, s), 8.97 (1 H, s), 8.46 (1 H, d, $J = 5.1$ Hz), 8.42 (1 H, d, $J = 8.6$ Hz), 8.10 (1 H, br s), 7.85 (1 H, d, $J = 5.1$ Hz), 7.51 (1 H, d, $J = 8.6$ Hz), 4.83 (1 H, m), 4.57 (2 H, s), 3.74 (2 H, t, $J = 6.0$ Hz), 2.88 (2 H, t, $J = 6.0$ Hz), 2.60–2.66 (2 H, m), 1.93–2.02 (4 H, m), 1.67 (1

H, m), 1.48 (9H, s), 1.22–1.34 (2 H, m), 1.06 (3H, d, $J = 6.4$ Hz). HRMS (ESI) m/z : calculated for $[\text{M} + \text{H}]^+$ 514.2925, found 514.2928.

9-((1*r*,4*r*)-4-Methylcyclohexyl)-*N*-(5,6,7,8-tetrahydro-1,6-naphthyridin-2-yl)-9*H*-pyrido[4',3':4,5]pyrrolo[2,3-*d*]pyrimidin-2-amine (73). To a suspension of **72** (4.65 g, 9.05 mmol) in MeOH (30 mL) were added concentrated HCl (6.74 mL) and water (14 mL). The mixture thus obtained was stirred at room temperature overnight. Analysis by HPLC-MS indicated that the reaction was complete. Then 50% NaOH in water (4.8 mL) was added at 0 $^\circ\text{C}$ to the reaction mixture to adjust the pH value to 9. The precipitated yellow solid was collected by filtration, rinsed with water (25 mL), and air-dried for 3 days to give compound **73** (3.75 g, 100% yield). ^1H NMR (400 MHz, CDCl_3) δ ppm 9.08 (1 H, s), 8.96 (1 H, s), 8.50 (1 H, d, $J = 5.3$ Hz), 8.34 (1 H, d, $J = 8.4$ Hz), 8.03 (1 H, br s), 7.84 (1 H, d, $J = 5.3$ Hz), 7.41 (1 H, d, $J = 8.4$ Hz), 4.71 (1 H, m), 4.04 (2 H, s), 3.26 (2 H, t, $J = 6.0$ Hz), 2.89 (2 H, t, $J = 6.0$ Hz), 2.53–2.69 (2 H, m), 2.02 (2 H, s), 1.95–2.00 (3 H, m), 1.25–1.29 (3 H, m), 1.07 (3 H, d, $J = 6.5$ Hz). HRMS (ESI) m/z : calculated for $[\text{M} + \text{H}]^+$ 414.2401, found 414.2404.

2,5-Dioxopyrrolidin-1-yl 2-acetoxyacetate (74). A 3-neck round-bottom flask equipped with a mechanical stirrer, thermocouple, and addition funnel with nitrogen inlet was charged with *N*-hydroxysuccinimide (211 g, 1.83 mol) and DCM (2.25 L) at room temperature, resulting in a suspension. Pyridine (178 mL, 2.2 mol) was added in one portion with no change in the internal temperature. A solution of acetoxyacetyl chloride (197 mL, 1.83 mol) in DCM (225 mL) was added dropwise over 60 min, and the temperature rose to 35 $^\circ\text{C}$. Stirring was continued at room temperature for 2.5 h. The stirring was stopped, and the reaction mixture was washed with water (1 L), 1 N HCl (2 L), and brine (1 L). The organic layer was concentrated under vacuum and azeotroped with toluene (1 L) to obtain compound **74** as a white solid (367 g, 93% yield). ^1H NMR (400 MHz, CDCl_3) δ ppm 4.96 (2 H, s), 2.86 (4 H, s), 2.19 (3 H, s) ppm. LCMS m/z : 238.0 $[\text{M} + \text{Na}]^+$.

2-(2-((9-((1*r*,4*r*)-4-Methylcyclohexyl)-9*H*-pyrido[4',3':4,5]pyrrolo[2,3-*d*]pyrimidin-2-yl)amino)-7,8-dihydro-1,6-naphthyridin-6(5*H*)-yl)-2-oxoethyl acetate (75). To a suspension of **73** (827 mg, 2.0 mmol) in chloroform (10 mL) were added diisopropylethylamine (258 mg, 348 μL , 2.0 mmol) and **74** (560 mg, 2.6 mmol). The reaction mixture thus obtained was stirred at room temperature for 30 min, whereupon the mixture became a yellow solution. HPLC-MS analysis indicated that the reaction was complete. The reaction mixture was concentrated. MeOH (5 mL) and water (6 mL) were added to form a slurry, which was stirred at room temperature for 1 h. The solid was collected by filtration to give compound **75** as a light-yellow solid (1.04 g, 98% yield). ^1H NMR (400 MHz, CDCl_3 , rotamers) δ ppm 9.11 (1 H, s), 8.98 (1 H, s), 8.52 (1 H, d, $J = 5.3$ Hz), 8.40–8.49 (1 H, m), 8.10–8.21 (1 H, m), 7.86 (1 H, d, $J = 5.3$ Hz), 7.45–7.57 (1 H, m), 4.82–4.90 (2 H, m), 4.65–4.80 (2 H, m), 4.59 (1 H, m), 3.97 (1 H, t, $J = 5.9$ Hz), 3.75 (1 H, t, $J = 5.9$ Hz), 2.93–3.08 (2 H, m), 2.52–2.69 (2 H, m), 2.22 (3 H, s), 1.97–2.03 (4 H, m), 1.20–1.37 (2 H, m), 1.08 (3 H, d, $J = 6.5$ Hz). HRMS (ESI) m/z : calculated for $[\text{M} + \text{H}]^+$ 514.2561, found 514.2563.

2-Hydroxy-1-(2-((9-((1*r*,4*r*)-4-methylcyclohexyl)-9*H*-pyrido[4',3':4,5]pyrrolo[2,3-*d*]pyrimidin-2-yl)amino)-7,8-dihydro-1,6-naphthyridin-6(5*H*)-yl)ethanone (28). To a solution of **75** (514 mg, 1.0 mmol) in DCM (7.5 mL) and MeOH (2.5 mL) was added 0.5 M sodium methoxide solution in MeOH (0.30 mL, 0.15 mmol), and the reaction mixture was stirred at room temperature for 1 h, monitored using LCMS. Upon completion, the reaction mixture was concentrated. The residue was treated with EtOH (5 mL) and water (10 mL) to provide a solid which was collected by filtration, washed with water, and dried in a vacuum oven at 55 $^\circ\text{C}$ overnight to give compound **28** as a white solid (468 mg, 99% yield). ^1H NMR (500 MHz, acetic acid- d_4 , 373 K) δ ppm 9.43 (1 H, s), 9.35 (1 H, s), 8.63 (1H, d, $J = 6.0$ Hz), 8.40 (1 H, d, $J = 6.0$ Hz), 8.33 (1 H, d, $J = 8.5$ Hz), 7.76 (1 H, d, $J = 8.5$ Hz), 4.90 (1 H, m), 4.77 (2 H, br s), 4.46 (2 H, br s), 3.88 (2 H, br s), 3.10 (2 H, t, $J = 5.4$ Hz), 2.68 (2 H, dq, $J = 12.7, 3.3$ Hz), 2.06–2.13 (2 H, m), 1.99–2.03 (2 H, m), 1.70–1.80 (1 H, m), 1.31–1.43 (2 H, m), 1.09 (3H, d, $J = 6.5$ Hz). HRMS (ESI) m/z : calculated for $[\text{M} + \text{H}]^+$ 472.2455, found 472.2461.

FLT3 Kinase Assay. The inhibitory activity of FLT3 was determined using a time-resolved fluorescence resonance energy transfer (TR-FRET) assay. The FLT3 enzyme (GST-fused human FLT3 cytoplasmic domain, amino acids 564–993) was purchased from Carna Biosciences (Natick, MA). An ULIGHT-labeled synthetic peptide (ULIGHT-JAK1, PerkinElmer, Waltham, MA) derived from human Janus kinase 1 (amino acids 1015–1027) was used as the phosphoacceptor substrate. The FLT3 assay was conducted in a 384-well white OptiPlate (PerkinElmer) in a total volume of 20 μ L. The reaction mixture contained 50 nM ULIGHT-JAK1, 116 μ M ATP (equal to K_m), 0.5 nM FLT3, and serially diluted test compounds in a reaction buffer of 50 mM Hepes, pH 7.6, 1 mM EGTA, 10 mM MgCl₂, 2 mM DTT, and 0.005% Tween 20. The reaction was allowed to proceed for 1 h at room temperature and stopped by adding 20 μ L of 20 mM EDTA and 4 nM LANCE Eu-W1024 antiphospho-tyrosine antibody (PerkinElmer) in LANCE detection buffer (PerkinElmer). The plates were incubated at room temperature for 2 h after addition of detection reagents and were then read on an Envision multimode reader (PerkinElmer). Fluorescence signals measured at 615 nm (8.5 nm bandwidth) and 665 nm (7.5 nm bandwidth) with a 60 μ s delay after excitation at 320 nm (75 nm bandwidth). The signal ratio at 665/615 nm (APC/Eu) was used in all data analyses. IC₅₀ values were obtained by analyzing competition curves using a four-parameter sigmoidal model in GraphPad Prism v5.01 (GraphPad).

CDK Kinases Assay. CDK4/Cyclin D₁, CDK6/Cyclin D₁, CDK1/Cyclin B, and CDK2/Cyclin A were purchased from Cell Signaling Technology (Danvers, MA). For CDK4 and CDK6 kinase assays, Rb (amino acids 773–928), and histone H1 were from Millipore (Bedford, MA) and used as substrate for CDK4/6 and CDK1/2, respectively. [³³P]-ATP was purchased from PerkinElmer (Shelton, CT). Assays were performed in 96-well filter plates (MSDVN6B50, Millipore, Bedford, MA) with a final volume of 100 μ L, containing 1 μ g Rb, 25 ng CDK4/cyclin D₁, 25 μ M ATP, 1 μ Ci [³³P]-ATP, and compound in kinase reaction buffer (20 mM Tris-HCl, pH 7.4, 10 mM magnesium chloride, 5 mM β -glycerophosphate, 1 mM dithiothreitol, and 0.1% bovine serum albumin). Plates with reaction mix were incubated at room temperature for 60 min, and reactions were terminated by addition of 200 μ L of 20% trichloroacetic acid. Wells were washed with 200 μ L of 10% trichloroacetic acid and left to dry at room temperature. The bottom of the plates were sealed with tape, and 100 μ L of MicroScint-20 scintillation cocktail (PerkinElmer, Shelton, CT) were added to each well. Plates were read on a TopCount (PerkinElmer, Shelton, CT) to determine radioactive incorporation. IC₅₀ values were calculated by nonlinear regression curve fitting using GraphPad Prism v5.01 (GraphPad).

Cell Growth Inhibition Assay. Cell growth was measured by a DNA synthesis assay. Cells were seeded in a 96-well Cytostar T plate (GE Healthcare Biosciences, Piscataway, NJ) at a density of 5×10^3 cells/well in a total volume of 160 μ L. The plates were incubated overnight to allow cells to attach. Test compounds were serially diluted into the plate (20 μ L/well), and 20 μ L/0.1 μ Ci of [¹⁴C]-thymidine (GE Healthcare Biosciences, Piscataway, NJ) were added to each well. Isotope incorporation was determined using a β plate counter (Wallac, Gaithersburg, MD) after a further 72 h. IC₅₀ values were determined as described above.

Analysis of pSTAT5 and pRb in Vitro. To determine levels of pSTAT5 and pRb, cells were seeded in a 96-well cell culture plate at a density of 5000–10000 cells per well in a total volume of 180 μ L and incubated overnight in medium containing 10% fetal bovine serum (Life Technologies, Rockville, MD). Then 20 μ L of serially diluted compounds were added to each well the next day. Cell lysates were harvested after 24 h and pSTAT5 or pRb was quantified using assay kits for pSTAT5 (Tyr694)/total STAT5 and pRb (Ser780)/total Rb (Meso Scale Discovery) following the manufacturer's protocols. Finally, 10 μ g of total protein from each sample was analyzed.

Apoptosis Assay. Apoptosis of the AML cells treated with compounds was assayed by using a Vybrant Apoptosis Assay Kit no. 9 following the manufacturer's protocol (Invitrogen, catalogue no. V35113). Briefly, the MOLM13, MOLM13^{SR}, or U937 cells in exponential growth phase were seeded into a 6-well plate at 5×10^5

cells per well and treated with compounds at indicated concentrations for 24 h. Cells were then stained with the reagents in the kit and analyzed by flow cytometry. The Sytox Green fluorescence versus APC fluorescence dot plot shows resolution of live, apoptotic and dead cells, which were quantified using Flowjo software.

Sorafenib-Resistant MOLM13 Cells. Sorafenib resistant MOLM13 (MOLM13^{SR}) was isolated by passing the cells in growth medium containing increasing concentrations of sorafenib (1–1000 nM) over 3–4 months. The resistant cells were cloned by limiting dilution. RNA was isolated from each clone, and cDNA was sequenced to identify FLT3 kinase domain mutations.

Xenograft Tumor Models. CrTac:NCR-Foxn1tm (NCR) nude mice were treated with ip injection of 100 μ L of antisialo GM (WAKO Chemicals) antibody to abolish NK activity and allow for enhanced growth of subsequently inoculated tumor cells. The following day, 7.5 million MOLM13 or U937 tumor cells in PBS were formulated as a 1:1 mixture with matrigel (BD Biosciences) and injected into the subcutaneous space on the right flank of the mice. Tumors were measured with PRO-MAX electronic digital caliper (Japan Micrometer Mfg. Co. LTD), and the mice were weighed every other day prior to each tumor measurement. Tumor volumes were calculated as follows: tumor volume (mm³) = [(W² × L)/2], where width (W) is defined as the smaller of the two measurements and length (L) is defined as the larger of the two measurements. Tumor growth inhibition (TGI) is calculated as $100 - [(measured - initial volume)/(control - initial volume) \times 100]$.

Statistical Analysis of Tumor Growth in Vivo. Tumor volumes are expressed as means plus or minus standard errors and plotted as a function of time. Statistical significance of observed differences between growth curves was evaluated by repeated measures analysis of covariance of the log transformed tumor volume data with Dunnett adjusted multiple comparisons. The analysis was done using SAS proc mixed with model effects of baseline log tumor volume, day, treatment, and day-by-treatment interaction; a repeated statement where day was a repeated value, animal the subject, and a Toeplitz covariance structure; and an lsmeans statement to do a Dunnett analysis comparing the control group to the other treatment groups. The data was log transformed because larger volumes tended to have larger variances, and baseline log tumor volume was included as a covariate in the model to account for possible pretreatment tumor volume differences. All statistical calculations were made through the use of JMP software v7.0 interfaced with SAS v9.1 (SAS Institute Inc., Cary, NC).

Analysis of pRb and pSTAT5 in Tumor Samples. Tumors were harvested by dissection and snap-frozen. Frozen tumors were weighed and lysed in 150 mM NaCl, 20 mM Tris pH 7.5, 1 mM EDTA, 1 mM EGTA, 1% Triton-X-100, and 2× protease and phosphatase inhibitors (Meso Scale Discovery) at twice the volume of tumor mass. Samples were processed on a Genogrinder (Spec SamplePrep) and shaken twice for 30 s at 1200 rpm with cooling on ice between shaking. Samples were then centrifuged at 1200 rpm, and cleared lysates were analyzed using assay kits for phosphorylated STAT5 (Tyr694), total STAT5a and b, phosphorylated Rb (Ser780)/total Rb, and total p38^{MAPK}.

X-ray Crystallography. The CDK6-Vcyclin complex was expressed and crystallized, using minor modifications on the methods described by Lu and Schulze-Gahmen.²⁹ In short, the CDK6 and Vcyclin proteins were expressed separately in baculovirus infected Hi5 cells. The proteins were mixed, and the complex was purified. The purified complex was concentrated to 10–15 mg/mL, and unliganded CDK6-Vcyclin was crystallized from 10 mM Tris pH 7.9, 100 mM calcium acetate, 10 mM DTT, 8–12% PEG 3350, and 100 mM NDSB-201. Crystals were soaked with 0.25 mM compound 1 and cryoprotected with glycerol prior to flash cooling. A 2.9 Å X-ray diffraction data set was collected at beamline 5.0.2 at the Berkeley Advanced Light Source and processed with iMOSFLM.³⁰ The structure was solved by molecular replacement with MOLREP³¹ using 2EUF as the search model. Final refinement and model building were carried out using PHENIX³² and Coot,³³ respectively. Atomic

coordinates have been deposited in the RCSB Protein Data Bank under accession code 4P41.

■ ASSOCIATED CONTENT

■ Supporting Information

POC kinase selectivity data of **28**, K_d data for **28** for the set of kinases with POC less than 20 from the initial POC screen, terminal exposure levels of **28** in the MOLM13 xenograft model, and average body weights for the **28** treated mouse group in the MOLM13 xenograft model. This material is available free of charge via the Internet at <http://pubs.acs.org>.

Accession Codes

The coordinates of **1** with CDK6 have been deposited in the PDB with accession code 4P41.

■ AUTHOR INFORMATION

Corresponding Author

*Phone: 650-244-2501. E-mail: zhihongl@amgen.com.

Notes

The authors declare no competing financial interest.

■ ACKNOWLEDGMENTS

We thank David Chaw for assistance of NMR spectra, Guifen Xu for bioanalytical support, Simon Wong for determination of CYP IC₅₀ values, and Dhanashri Bagal and Iain Campuzano for determination of high-resolution mass spectra. We also thank Xiaolin Hao for useful discussion.

■ ABBREVIATIONS USED

AML, acute myeloid leukemia; ATP, adenosine triphosphate; AUC, area under curve; CDK4, cyclin-dependent kinase 4; CL, clearance; C_{max} , maximum concentration; CYP3A4, cytochrome p450 3A4; DCM, dichloromethane; DIPEA, *N,N*-diisopropylethylamine; DMAP, dimethylaminopyridine; DMF, dimethylformamide; dppf, ferrocene,1,1'-bis(diphenylphosphino)-; ED, effective dose; EDTA, ethylenediamine-*N,N,N,N'*-tetraacetic acid; EGTA, ethylene glycol bis(2-aminoethyl ether)-*N,N,N,N'*-tetraacetic acid; *F*, bioavailability; Fe(acac)₃, tris(acetylacetonato) iron(III); FLT3, FMS-like tyrosine kinase 3; hERG, human ether-à-go-go-related gene; IC₅₀, half-maximal inhibitory concentration; KHMDs, potassium bis(trimethylsilyl)amide; LiHMDs, lithium hexamethyldisilazide; LiTMP, 1-lithio-2,2,6,6-tetramethylpiperidine; NIS, *n*-iodosuccinimide; NMP, *N*-methyl-2-pyrrolidone; PBS, phosphate buffered saline; PI3K, phosphatidylinositol 3 kinase; PK, pharmacokinetic; PPTS, pyridinium *p*-toluenesulfonate; Rb, retinoblastoma protein; SAR, structure-activity relationship; TEA, triethylamine; TFA, trifluoroacetic acid; THF, tetrahydrofuran; TLC, thin layer chromatography; V_{ss} , volume of distribution; XantPhos, 4,5-bis(diphenylphosphino)-9,9-dimethylxanthene; X-Phos, 2-dicyclohexylphosphophino-2'4'6'-trisopropylbiphenyl

■ REFERENCES

- (1) *Cancer Facts & Figures 2013*; American Cancer Society: Atlanta, 2013.
- (2) Birg, F.; Courcoul, M.; Rosnet, O.; Bardin, F.; Pebusque, M. J.; Marchetto, S.; Tabilio, A.; Mannoni, P.; Birnbaum, D. Expression of the FMS/KIT-like gene FLT3 in human acute leukemia of the myeloid and lymphoid lineages. *Blood* **1992**, *80*, 2584–2593.
- (3) Carow, C. E.; Levenstein, M.; Kaufmann, S. H.; Chen, J.; Amin, S.; Rockwell, P.; Witte, L.; Borowitz, M. J.; Civin, C. I.; Small, D.

Expression of the hematopoietic growth factor receptor FLT3 (STK-1/Flk2) in human leukemia. *Blood* **1996**, *87*, 1089–1096.

(4) Drexler, H. G. Expression of FLT3 receptor and response to FLT3 ligand by leukemic cells. *Leukemia* **1996**, *10*, 588–599.

(5) Thiede, C.; Steudel, C.; Mohr, B.; Schaich, M.; Schakel, U.; Platzbecker, U.; Wermke, M.; Bornhauser, M.; Ritter, M.; Neubauer, A.; Ehninger, G.; Illmer, T. Analysis of FLT3-activating mutations in 979 patients with acute myelogenous leukemia: association with FAB subtypes and identification of subgroups with poor prognosis. *Blood* **2002**, *99*, 4326–4335.

(6) Pratz, K. W.; Levis, M. J. Bench to bedside targeting of FLT3 in acute leukemia. *Curr. Drug Targets* **2010**, *11*, 781–789.

(7) Kindler, T.; Lipka, D. B.; Fischer, T. FLT3 as a therapeutic target in AML; still challenging after all these years. *Blood* **2010**, *9*, 5089–5102.

(8) Smith, C. C.; Wang, Q.; Chin, C.; Salerno, S.; Damon, L. E.; Levis, M. J.; Perl, A. E.; Travers, K. J.; Wang, S.; Hunt, J. P.; Zarrinkar, P. P.; Schadt, E. E.; Kasarskis, A.; Kuriyan, J.; Shah, N. P. Validation of ITD mutations in FLT3 as a therapeutic target in human acute myeloid leukaemia. *Nature* **2012**, *485*, 260–263.

(9) Knapper, S. FLT3 inhibition in acute myeloid leukaemia. *Br. J. Haematol.* **2007**, *138*, 687–699.

(10) Wang, L.; Wang, J.; Blaser, B. W.; Duchemin, A. M.; Kusewitt, D. F.; Liu, T.; Caligiuri, M. A.; Briesewitz, R. Pharmacologic inhibition of CDK4/6: mechanistic evidence for selective activity or acquired resistance in acute myeloid leukemia. *Blood* **2007**, *110*, 2075–2083.

(11) Drexler, H. G. Review of alterations of the cyclin-dependent kinase inhibitor INK4 family genes p15, p16, p18 and p19 in human leukemia-lymphoma cells. *Leukemia* **1998**, *12*, 845–859.

(12) Malumbres, M.; Barbacid, M. Cell cycle, CDKs and cancer: a changing paradigm. *Nature Rev. Cancer* **2009**, *9*, 253–266.

(13) Li, Z.; Dai, K.; Keegan, K.; Ma, J.; Ragains, M.; Kaizerman, J.; McMinn, D.; Fu, J.; Fisher, B.; Gribble, M. et al. CDK4/FLT3 dual inhibitors as potential therapeutics for acute myeloid leukemia. In *Drug Discovery and Lead Optimization*; Proceedings of the American Association for Cancer Research, AACR Annual Meeting 2013, Washington, DC, April 6–10, 2013; Abstract 2351, p 575.

(14) All software programs used for molecular modeling are from Schrödinger (New York, NY). The homology model for FLT3 with the activation loop in the DFG-in conformation was built with cKit as the scaffold (PDB 1PKG) using the Prime module. Compound **1** was modeled into the ATP binding site of the FLT3 model using Glide. Protein representations were prepared via PyMOL 1.5.0.5.

(15) Malumbres, M.; Pevarello, P.; Barbacid, M.; Bischoff, J. R. CDK inhibitors in cancer therapy: What is next? *Trends Pharmacol. Sci.* **2008**, *29*, 16–21.

(16) Detailed docking studies of our compound to the CYP3A4 active site will be published elsewhere in due course.

(17) Takács-Novák, K.; Szasz, G. ion pair partition of quaternary ammonium drugs: the influence of counter ions of different lipophilicity, size, and flexibility. *Pharm. Res.* **1999**, *16*, 1633–1638.

(18) KINOMEScan Assay Platform; DiscoveRx Corporation: Fremont, CA; <http://www.discoverx.com/technologies-platforms/competitive-binding-technology/kinomescan-technology-platform>.

(19) Sorafenib and palbociclib were purchased from AdooQ BioScience (Irvine, CA).

(20) More detailed in vitro and in vivo studies of **28** and its abilities to simultaneously inhibit CDK4 and FLT3 and suppress mutations in FLT3 will be published elsewhere in due course.

(21) Zuccotto, F.; Ardini, E.; Casale, E.; Angiolini, M. Through the “gatekeeper door”: Exploiting active kinase conformation. *J. Med. Chem.* **2010**, *53*, 2681–2694.

(22) Liu, Y.; Gray, N. S. Rational design of inhibitors that bind to inactive kinase conformations. *Nature Chem. Biol.* **2006**, *2*, 358–364.

(23) FLT3 apo structure (PDB 1RJB) used for DFG-out kinase with Sorafenib modeled with Glide. FLT3 DFG-in homology model (cKIT, PDB 1PKG) used to model **28**.

(24) The deference in inhibition between pRb and pSTAT5 at 24 h time point in 75 and 150 mg/kg dosing groups is due to the fact that

total STAT5 was stable with the compound treatment, while total Rb decreased with the compound treatment. At 24 h at doses of 150 and 75 mg/kg, compound concentrations in plasma went down, so STAT5 phosphorylation was not inhibited, and back to normal. In contrast, although Rb phosphorylation was not inhibited at 24 h, but because total Rb level was low, pRb appeared low compared to vehicle.

(25) Syntheses of certain substituted cycloalkane derivatives (e.g., **8**, **9**, and **14**) employed minor modifications of the general route depicted in Scheme 1, such as permutation of steps (**14**) or inclusion of additional protecting group manipulations (**8**, **9**). These deviations from the mainstream approach are detailed in the experimental procedures for the relevant compounds.

(26) The exocyclic amine nitrogen was arbitrarily numbered as 1' in this scheme to facilitate unambiguous reference to this atom in the discussion. IUPAC names for the fully elaborated derivatives number this position differently.

(27) Gribble, G. W.; Saulnier, M. G. Regioselective ortho lithiation of halopyridines. *Tetrahedron Lett.* **1980**, *21*, 4137–4140.

(28) Marsais, F.; Queguiner, G. Review on the metallation of p-deficient heteroaromatic compounds. Regioselective ortho-lithiation of 3-fluoropyridine: directing effects and application to synthesis of 2,3- or 3,4-disubstituted pyridines. *Tetrahedron* **1983**, *39*, 2009–2021.

(29) Liu, H.; Schulze-Gahmen, U. Toward understanding the structural basis of cyclin-dependent kinase 6 specific inhibition. *J. Med. Chem.* **2006**, *49*, 3826–3831.

(30) Batty, T. G. G.; Kontogiannis, L.; Johnson, O.; Powell, H. R.; Leslie, A. G. W. iMOSFLM: a new graphical interface for diffraction-image processing with MOSFLM. *Acta Crystallogr., Sect. D: Biol. Crystallogr.* **2011**, *67*, 271–281.

(31) Winn, M. D.; Ballard, C. C.; Cowtan, K. D.; Dodson, E. J.; Emsley, P.; Evans, P. R.; Keegan, R. M.; Krissinel, E. B.; Leslie, A. G.; McCoy, A.; McNicholas, S. J.; Murshudov, G. N.; Pannu, N. S.; Potterton, E. A.; Powell, H. R.; Read, R. J.; Vagin, A.; Wilson, K. S. Overview of the CCP4 suite and current developments. *Acta Crystallogr., Sect. D: Biol. Crystallogr.* **2011**, *67*, 235–242.

(32) Adams, P. D.; Afonine, P. V.; Bunkóczi, G.; Chen, V. B.; Davis, I. W.; Echols, N.; Headd, J. J.; Hung, L.-W.; Kapral, G. J.; Grosse-Kunstleve, R. W.; McCoy, A. J.; Moriarty, N. W.; Oeffner, R.; Read, R. J.; Richardson, D. C.; Richardson, J. S.; Terwilliger, T. C.; Zwart, P. H. PHENIX: a comprehensive Python-based system for macromolecular structure solution. *Acta Crystallogr., Sect. D: Biol. Crystallogr.* **2010**, *66*, 213–221.

(33) Emsley, P.; Lohkamp, B.; Scott, W. G.; Cowtan, K. Features and development of Coot. *Acta Crystallogr., Sect. D: Biol. Crystallogr.* **2010**, *66*, 486–501.